# EVALUATION OF THE AZINOMYCIN B BIOSYNTHETIC PATHWAY: THE AZABICYCLE FORMATION

A Dissertation

by

RACHEL POKEI LEE

Submitted to the Office of Graduate and Professional Studies of
Texas A&M University
in partial fulfillment of the requirements for the degree of

MASTER OF SCIENCE

| | |
|---|---|
| Chair of Committee, | Coran M. H. Watanabe |
| Committee Members, | Tadhg P. Begley |
| | Deborah A. Siegele |
| Head of Department, | David H. Russell |

May 2014

Major Subject: Chemistry

## ABSTRACT

Azinomycin B is an antitumor agent isolated from the soil bacteria *Streptomyces sahachiroi*. The complex molecular structure of azinomycin B contains a bioactive aziridine ring and an epoxide moiety, which are the major structural components responsible for the natural product's antitumor bioactivity. In this study, we attempt to characterize the early steps of azinomycin B's aziridine-containing azabicycle fragment biosynthesis and subsequently further elaborate on our existing knowledge on the overall biosynthesis of azinomycin B.

Previous attempt to characterize AziC2 suggested that the first step of azinomycin B's azabicycle fragment formation involves the transfer of L-glutamate, the amino-acid precursor, to downstream biosynthetic enzymes through the catalytic activity of a putative N-acetyltransferase (AziC2), which utilizes acetyl-CoA as a feasible acetyl group donor. Interestingly, by closely examining the azinomycin B's biosynthetic gene cluster and related homologs, we identified a previously uncharacterized protein AziW that may acts as an alternative acetyl group donor for AziC2. In addition, BLAST studies had proposed that AziC2 might potentially confer unrevealed phosphatase activity and function in conjunction with the novel AziW during the biosynthesis of azinomycin B's azabicyclic moiety. To characterize the relationship between AziC2 and AziW, we performed radiolabeled feeding studies. The result from these labeling experiments indicated that the C-terminal of AziW is independently phosphorylated via self-activation in the presence of ATP. Most importantly, this phosphorylation event occurs

prior to the transfer of L-glutamate by AziC2. These findings suggest that AziC2 only acts an acetyltransferase but not as a phosphatase towards AziW during the biosynthesis of azinomycin B's azabicycle fragment. In addition, our labeling experiments and feeding studies also confirmed the functions of AziC3 and AziC4 as kinase and reductase respectively. This dissertation also includes our ongoing progress with AziH1, AziH2 and AziH3 which are responsible for the formation of the aziridine ring. The potential interaction between AziW and its enzymatic partners may offer advanced insights on the regulation mechanism involved in the biosynthesis of azinomycin B and help decipher the complex enzymology that highlights the biosynthesis of related natural products.

## ACKNOWLEDGEMENTS

I would like to thank my labmates and mentors, especially Dr. Dinesh Simkahda and Dr. Huitu Zhang, for their advices and supports both inside and outside the lab. They made me feel like the lab is my second family. I also want to thank my labmates, Vishruth Gowda, Felix Yu and Hillary Agbo for their gratuity of suggestions and ideas. I wouldn't be able to successfully complete many of the challenges that I encountered during this research experience.

To professor Watanabe, I really appreciate the time she spent on guiding me and gave me the opportunity to participate in her research for the past two years. Under her motivation, I enjoyed being a graduate student as well as a researcher. Her endless backing allowed me to fulfill my project and successfully completed this dissertation. Additionally, I would like to thank the faculties who participated in my committee, professor Tadgh Begley and Deborah Siegele, for kindly advising me and providing me with the necessary supports.

Finally, to my family and my fiancé, thank you for their understanding and spiritual support while I am away from home.

## TABLE OF CONTENTS

## LIST OF FIGURES

Page

## LIST OF TABLES

## LIST OF SCHEMES

Page

# CHAPTER I

## INTRODUCTION: BIOSYNTHESIS OF NATURAL PRODUCT

### NATURAL PRODUCT OVER THE YEARS

For the past half-century, approximately 50% of small molecules that exhibit antitumor activities are derived from natural products (Figure 1).[1] Early approach in screening large libraries of synthetic compounds for efficacy largely relied on combinatorial chemistry technology.[2] However, this combinatorial approach failed to yield a significant amount of new drugs during the past 30 years, with sorafenib/ Nexavar® as the only rare case of success. Consequently, this led researchers to primarily focus on using smaller collections of structurally related compounds with defined natural product origins. As a result of this new approach, the majority of drugs discovered in the past decade are natural product derivations. In addition, natural product-derived compounds accounted for 50% of the total small molecule approved drugs in 2010 (Figure 2). Most importantly, the ongoing effort to exploit the clinical potential of nature's chemical reservoir continues to perpetuate the necessary development of more potent and nontoxic drugs for clinical use.

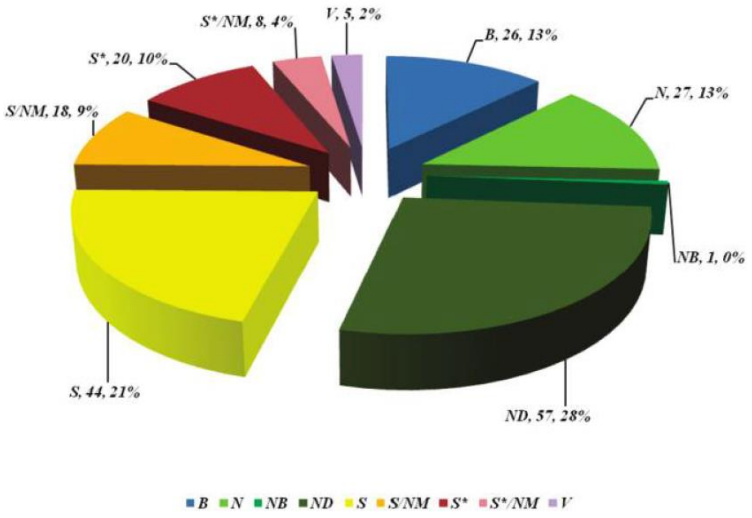


**Figure 1** The distribution of anticancer drugs from 1940s to 2010. Total number of drugs =206. N: Natural product; NB: Natural product- Botanical; ND: Natural product derivatives; S: Totally synthetic drug, often found by random screening/modification of an existing agent; S*: Totally synthetic drug but the pharmacophore is/ was from a natural product; V: Vaccine; B: Biological, includes peptide or protein isolated from an organism/cell line or biotechnologically produced in a surrogate host. Subcategory (NM: Natural product minic) **Adapted from** Newman *et al.* [1].

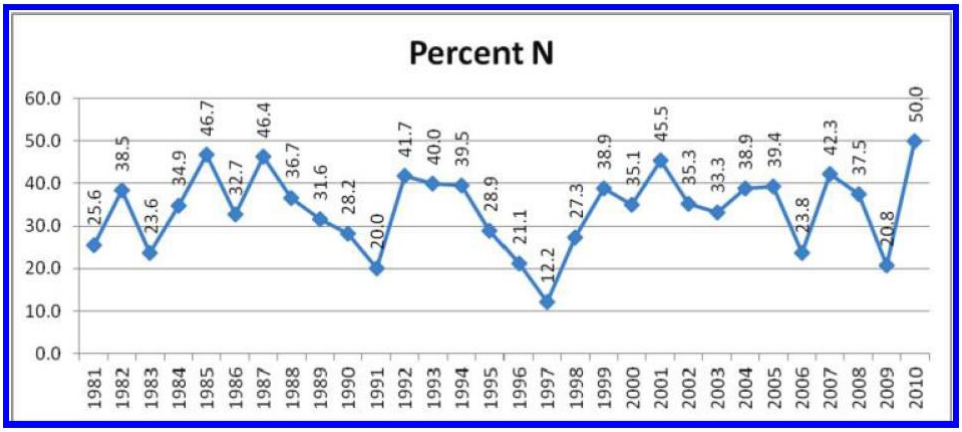


**Figure 2** The percentage of drugs in the N/NB/ND categories from 1981-2012. **Adapted from** Newman *et al.* [1].

Most of the novel therapeutic agents developed in the past decade are natural products or inspired by the structures of natural products. Figure 3 offers some examples

of drugs isolated from natural resources or structurally originated from natural products.[3] Many of these natural product-derived small molecules exhibit diverse and potent bioactivities. For example, taxol® (3**a**) is an antitumor drug isolated from the stem bark of Pacific yew tree, *Taxus breuifolia*.[4] This natural product effectively inhibits mitosis via microtubule over-stabilization.[5] On the other hand, rapamycin/ Sirolimus®(3**b**), produced by *Streptomyces hygroscopicus,* is routinely used as an antifungal antibiotic.[6] Simvastatin/ Zocor® (3**c**) is a structurally modified analog of the natural product lovastatin, a metabolite from *Aspergillus terreus*, and it acts as a hypolipidemic agent.[7] Finally, Cytarabine/ Depocyt® (3**d**), is a synthetic antitumor agent derived from metabolites of a marine organism *Cryptotheca crypta*.[8]

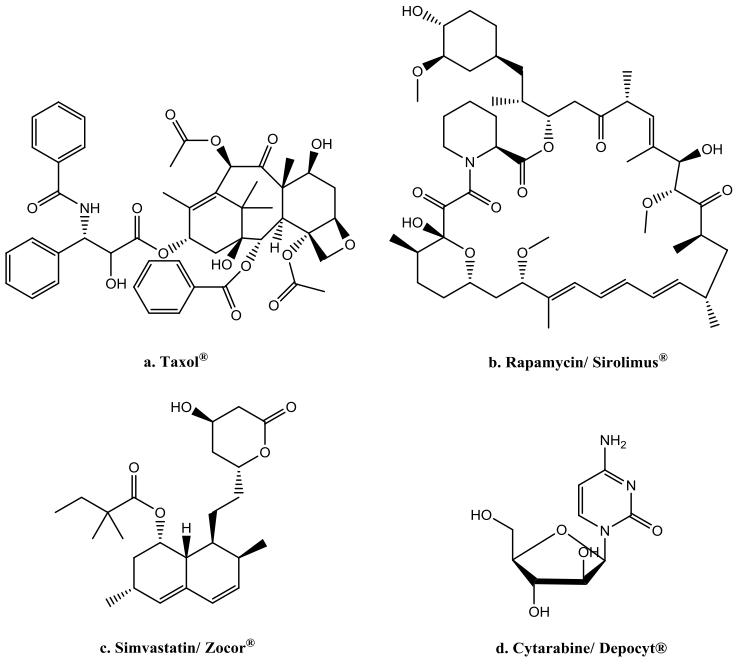


**Figure 3** Examples of drugs inspired by natural products. **a.** Taxol®; **b.** Rapamycin/ Sirolimus®; **c.** Simvastatin/ Zocor®; **d.** Cytarabine/ Depocyt®

## SYNTHETIC BIOLOGY OF NATURAL PRODUCTS

Natural products are produced by organisms through a devoted biosynthetic pathway and tailored by nature in response to different biological targets. Their chemical structures are usually very complex and require cellular modification that may not be replicable using synthetic methodology. Not only is organic synthesis of complex natural product as therapeutic agent very laborious and time-consuming, it may also generate harmful reaction side products and ultimately result in a very low yield. Therefore synthetic approach is not ideal and commercially unfeasible. In contrary, synthetic biology approach, where the site specific enzymatic reaction can eliminate complicated protection and deprotection steps in total synthesis; simple synthetic route can be used to replace redundant enzymes.

## THE HISTORY OF AZINOMYCINS

Azinomycin B (Figure 4), originally called carzinophilin A, was first isolated from *Streptomyces sahachiroi* by Hata *et al.* in Tokyo in 1954. Initially, this bacterial strain was found to inhibit a malignant tumor, Yoshida sarcoma, and prolong the lifespan in treated rats with the cancer.[9] Shortly after the discovery of the natural product, the clinical studies of carzinophilin A were reported.[10] Soon afterward, the advancement of isolation and spectroscopic technique led to the complete structural characterization of carzinophilin A (Figure 5). The molecular formula of carzinophilin A was first reported as $C_{60}H_{60}O_{21}N_6$, but later corrected to $C_{50}H_{58}O_{18}N_5$ by Tanaka *et al.*in 1959. They also reported the partial structure of carzinophilin A contains 3-methoxy-5-methylnaphthalene-2-carboxylic acid (5**a**) by fragmenting the molecule using alkaline

hydrolysis. [11-13] Onda *et al.* repeated the alkaline hydrolysis of carzinophilin A in 1971 and reassigned the substituents on the naphthoate moiety to give 3-methoxy-5-methylnaphthalene-1-carboxylic acid (5**b**).[14] In 1982, a more complete structure of carzinophilin A, as a dimerized molecule, is reported by Lown in congruent with his previous studies based on the natural product's DNA interstrand crosslinking properties (5**c**).[15] Further studies by Onda *et al.*in 1983 and 1984 suggested two more different structures (5**d, 5e**).[11, 16] In 1986, over 30 years after carzinophilin A was first isolated, the actual structure of carzinophilin A was finally determined by Yokoi *et al.* The result of this discovery gave rise to the existence of azinomycin B (5**f**). In addition to azinomycin B, other metabolites including azinomycin A and naphthoate derivatives, were also identified.[17]

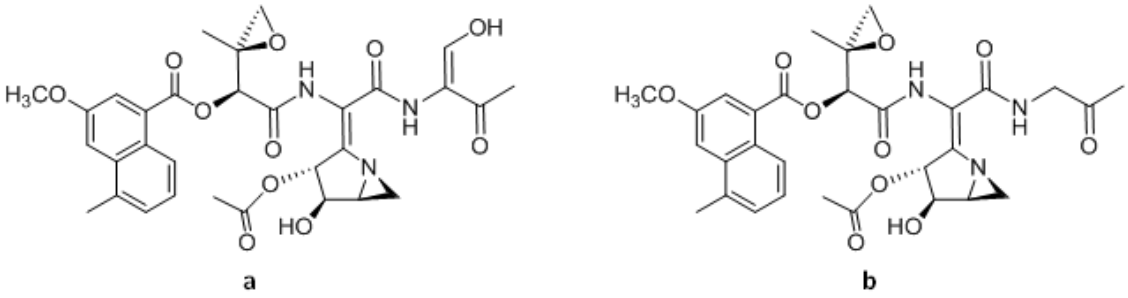


**Figure 4** Structure of the azinomycin B (a) and azinomycin A (b) isolated from *Streptomyces sahachiroi*.

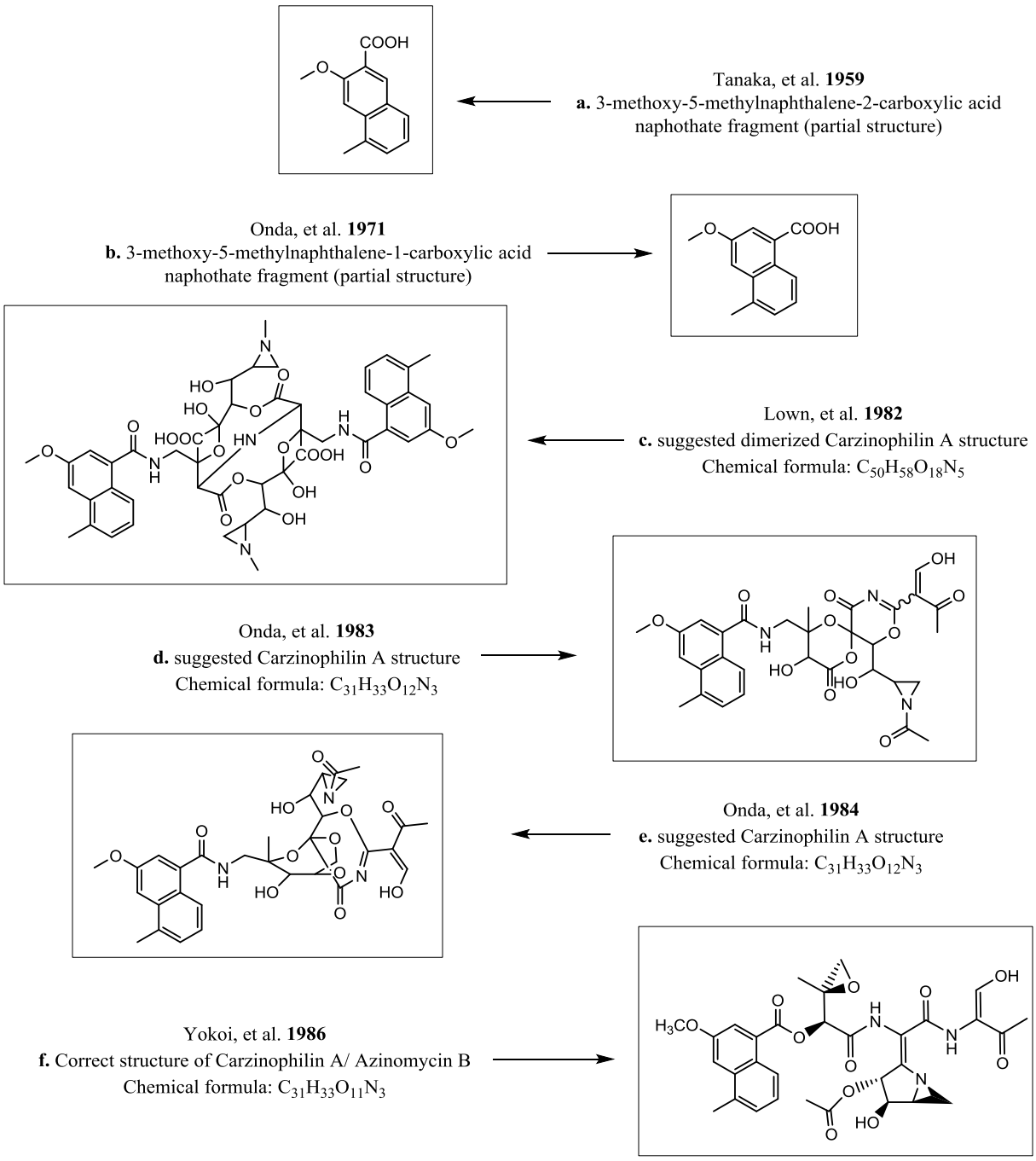


**Figure 5** Proposed structures for Carzinophilin A/ Azinomycin B.

## STREPTOMYCES, NATURAL PRODUCTS AND BIOSYNTHESIS

*Streptomycetes* are gram-positive soil dwelling bacteria that constitute the largest genus of *Actinobacteria*.[18] These filamentous fungus-like bacteria generate aerial branches to form spores with muddy odor. They consume plant materials and fungus for nutrients, and promote self-defense by secreting antibiotics during reproductive phase against invading pathogens/bacteria.[19] *Streptomycetes* produce numerous natural antibiotics and a wide range of bioactive secondary metabolites that can be used as anticancer drugs, antifungals and immunosupressants [6, 20, 21]. Majority of the antibiotics found in medical use are naturally-derived from *Streptomycetes*, such as neomycin from *S. fradiae*; streptomycin from *S. griseus*; and vancomycin from *S. orientalis*. The complete sequencing of the first *Streptomyces* genome in 2002 had encouraged the industry to employ Steptomycetes microorganism for secondary metabolites production to screen for active compounds.[22, 23] Since then, the biosynthetic pathways and the mode of action of these compounds had been heavily studied and researched. However, at times, potent therapeutic agents fell short in clinical application due to poor solubility and high toxicity. Consequently, studying the biosynthetic pathway of natural product will subsequently benefit future drug design in favor of improving the pharmacokinetics/pharmacodynamics of these compounds.[24]

## THE ANTITUMOR AGENT AZINOMYCIN B

Azinomycin A and azinomycin B (Figure 4), were not identified until they are re-isolated from *Streptomyces griseofuscus* in 1986.[25,26] These compounds are slightly different in structure but they sustain unique bioactivity. Current focus on azinomyzin B

is due to its significant cytotoxic effect. Cytotoxicity studies showed that azinomycin B is highly cytotoxic against the leukemia cell line L5178Y ($IC_{50}$ = 0.11µg/mL).[27] In other mouse model studies, treatment of azinoymcin B also led to increased life span (ILS) of 193% (32µg/kg) in P388 leukemia mouse models. In comparison to the chemotherapeutic mitomycin C (increased life span (ILS) of 204% (1mg/kg)), azinoymcin B proves to be more potent at a lower dosage.[28]

As a potent antitumor agent, azinomycin B binds to the major groove of DNA and introduces DNA interstrand cross-links.[29,30] As illustrated in Figure 6, this mode of interaction with double stranded DNA is responsible for its anti-tumor activity. The nitrogen N7 of a suitably disposed purine bases of DNA attacks the electrophilic carbon C10 of the aziridine ring system or the carbon C21 of the epoxide moiety in azinomycin B, which leads to DNA alkylation. Ultimately, this deadly interaction triggers damages in the double-strand that are not repairable.[31]

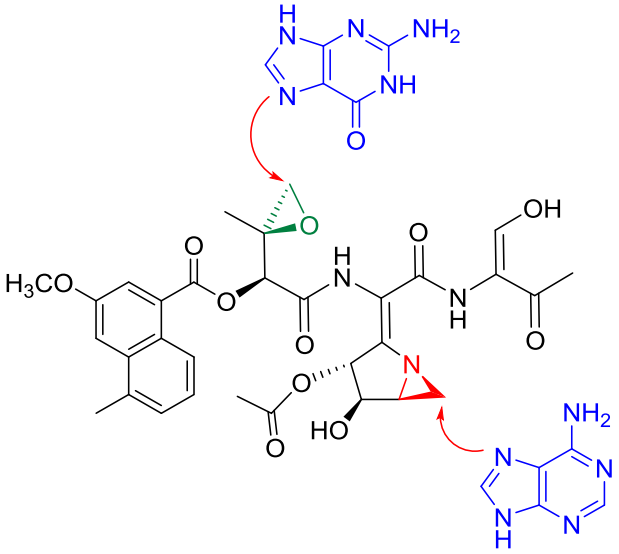


**Figure 6** Mode of action: DNA alkylation of azinomycin B.

## AZINOMYCIN B BIOSYNTHETIC PATHWAY

Aziridine-containing natural products are rare and fascinating secondary metabolites that. Specifically, azinomycin B is the only aziridine-containing natural products with its gene cluster completely published.[32] The aziridine functional group in azinomycin B is believed to contribute much to the natural product's cytotoxicity in living cells, making it an interesting candidate to study from the biosynthetic and functional perspective.

The first biosynthetic study of azinomycin B was carried out by Corre and Lowden via feeding labeled $^{13}$C-acetate precursors, including [1- or 2- or 1, 2-$^{13}$C]-acetate, into the fermentation cultures of *Streptomyces sahachiroi*. Azinomycin B, incorporated with the $^{13}$C label, was isolated and analyzed using $^{13}$C-NMR spectroscopy. The result confirmed the polyketide synthase-oriented naphthoate fragment is assembled from one acetyl-CoA and five malonyl-CoA units.[33] Further studies using synthetic naphthoic acids with deuterated methyl group showed that the formation of the naphthoate moiety is completed before integrating into the molecule.[34] The incorporation of the doubly-labeled [1, 2-$^{13}$C]-acetate into the enol fragment (2-$^{13}$C in C1 and C4; 1-$^{13}$C in C1 to C4) and the [1-$^{13}$C] acetyl group into C13 of the aziridine fragment, suggested threonine and α-ketoglutarate are possibly the building blocks of these moiety respectively.[33] When [U-$^{13}$C] threonine was supplied to the fermentation culture, the enol fragment was specifically labeled, which indicates threonine is the precursor of the keto-enol portion of azinomycin B. The epoxide moiety of azinomycin B was evaluated using [1-$^{13}$C]-valine derivatives and analyzed based on the relative $^{13}$C incorporation. L-

valine was finally validated as the precursor of the epoxide moiety where it undergoes a series of hydroxylation, transamination, and dehydration to form 3-methyl-2-oxobutenoate before ligating onto the final structure of azinomycin B (Figure 7).[35,36]

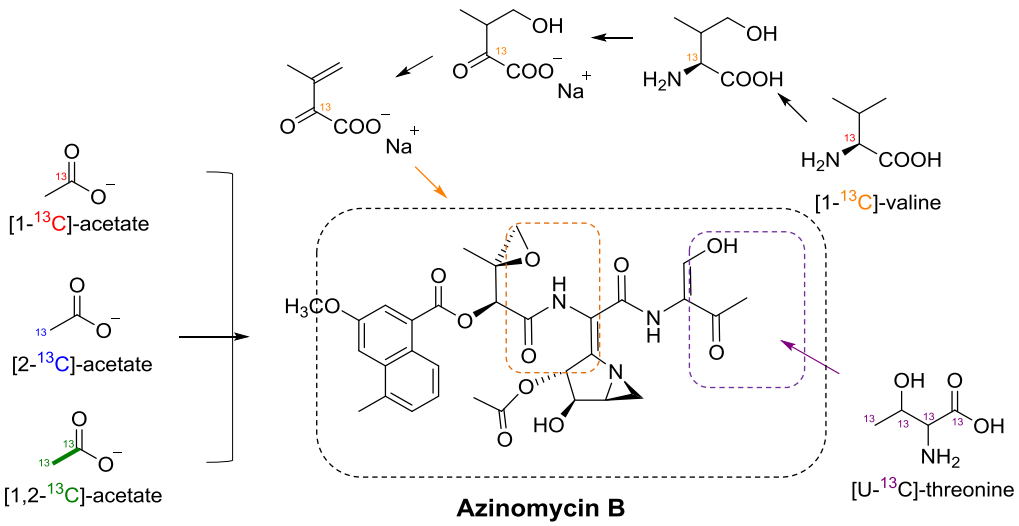


**Figure 7** Evaluation of the biosynthetic origins of azinomycin B.

In 2008, Zhao *et al.* successfully identified the biosynthetic gene cluster of azinomycin B using PCR screening. A library of *S. sahachiroi* genome was created and PCR probes were used to screen thousands of clones. By locating overlapped cosmids and using chromosome walking techniques, they revealed an 80kb DNA region representing the azinomycin B gene cluster (Figure 8). [32]

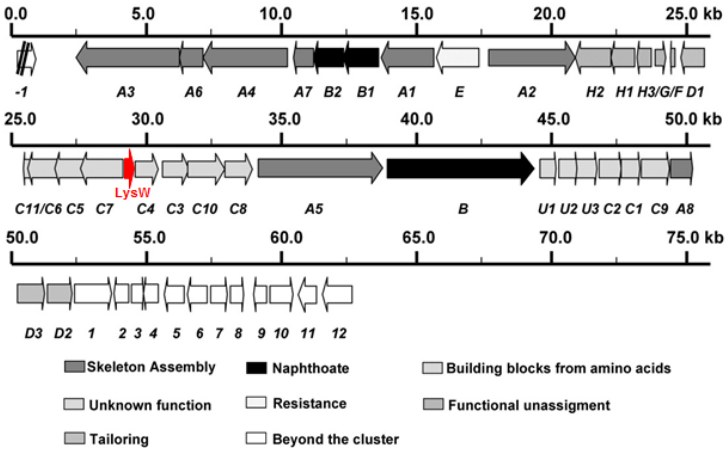


**Figure 8** The gene cluster of azinomycin B. **Adapted and modified from** Zhao *et al.* [32].

The genes encoding the building blocks of azinomycin B were proposed based on bioinformatics analysis. Sequence similarity and domain organization suggest *aziB* is the PKS gene responsible for the formation of 5-methyl-naphthoic acid. Modification of 5-methyl-naphthoic acid by *aziB1* and *aziB2* gives the final naphthoate fragment 3-methoxy-5-methyl-naphthoic acid. The formation of the azabicycle moiety may involve up to ten genes, *aziC2* to *azi11*, but the detailed mechanism in how the five-membered ring and the aziridine ring are formed still remains unknown. Different building blocks are joined together and tailored by the peptide carrier domain (PCP) encoded by the nonribosomal peptide synthetases (NRPS) genes, *aziA1* to *aziA5*. The biosynthetic pathway proposed by Zhao *et al.* is outlined in Figure 9. [32]

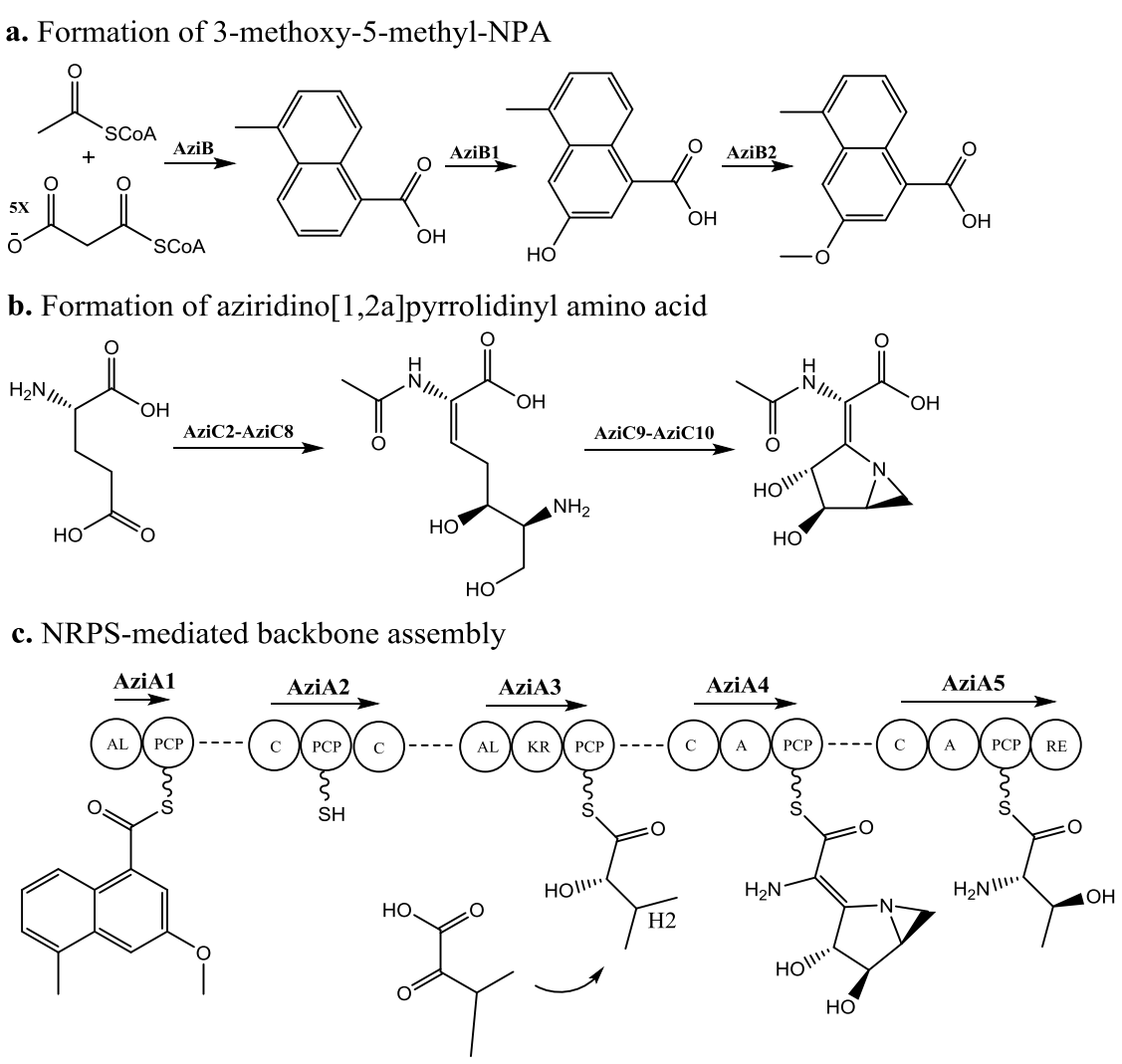


**Figure 9** Suggested biosynthetic pathway of azinomycin B fragments. AL: aldolase; PCP: peptide carrier protein; C: condensation; KR: ketoreductase; A: adenylation.

Enzymatic studies of the azinomycin B biosynthesis are ongoing after the publication of its gene cluster. According to an *in vivo* study by Ding *et al.*, heterologous expression of the PKS AziB confirmed the production of 5-methyl naphthoic acid. The use of the P450 hydroxylase AziB1 along with the O-methyltransferase AziB2 resulted in the formation of 3-hydroxy-5-methyl-naphthoic acid, as shown in both *in vivo* and *in*

*vitro* HPLC analysis. The NRPS AziA1 was found to activate the 3-methoxy-5-methyl-naphthoic acid by using ATP-[$^{32}$P]-PPi exchange study. [37] *aziR*, located outside the azinomycin B gene cluster, was characterized as a resistance protein through heterologous expression and the examination of in-cell protective effect.[38] Gene knockout study of *aziU1* through *aziU3* reduced azinomycin B production in fermentation media.[39] Up to this date, the effort to paint the entire picture of the azinomycin B biosynthesis is still ongoing.

**THE AZABICYCLE BIOSYNTHESIS**

Natural products consist of various kinds of three-membered ring structures, such as aziridine, cyclopropone and epoxide, which usually possess antibiotic and/or antitumor activities.[40-43] Ring opening of the strained ring system triggers site-specific electrophilic attack that results in DNA alkylation. Therefore, many researchers are interested in understanding how these strained bioactive structural moiety are chemically tolerated and biosynthetically made. In the case of azinomyicin B biosynthesis, the assembly of cyclopropane uses isoprenoid pyrophosphates as their building block. Intermolecular alkylation by prenyltransferase or intramolecular alkylation by terpene synthase release pyrophosphate and generate a carbocationic intermediate which undergoes electrophilic addition, rearrangements, and finally quenched to give the final cyclized product.[44-46] The P450-dependent epoxide formation involves oxygen bond cleavage to generate a cationic radical that reacts with the alkene. The change of Fe oxidation state stabilizes reactive radical species to achieve the incorporation. The catalytic cycle is regenerated by a water molecule. [46-49] Due to the rarity of gene cluster

published for aziridine-containing natural products, the aziridine formation is by far the least understood compare to the cyclopropane and epoxide moieties. Bicker and Fischer reported an observation that involves the sulfate donor, 3'-phosphoadenosine-5'-phosphosulfate (PAPS), in the pronethalol aziridine biosynthesis. The hydroxyl group is sulfated by PAPS via sulfotransferase. Sulfate is a better leaving group than the hydroxyl group and facilitates the aziridine ring closure (Figure 10).[50]

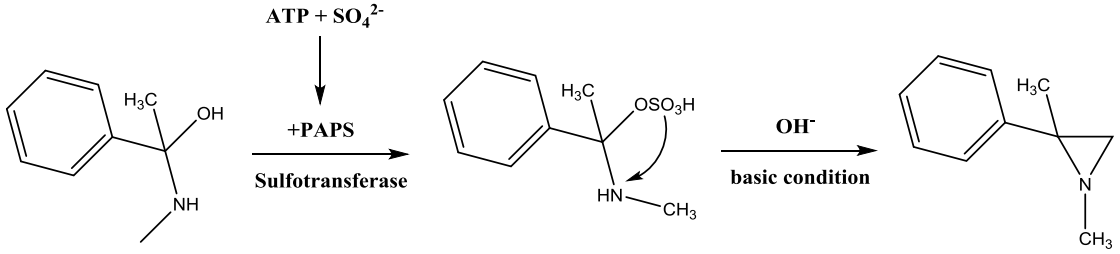


**Figure 10** The proposed PAPS-dependent aziridine formation.

# CHAPTER II

## AZIW, A PROTEIN INVOLVES IN THE AZABICYCLE BIOSYNTHESIS OF AZINOMYCIN B

### INTRODUCTION

The gene cluster of azinomycin B (Figure 8) is identified using heterologous expression studies in the host organism *Scaphirhynchus albus*. It discloses an iterative type I polyketide synthase (PKS) and five nonribosomal peptide synthetases (NRPS) responsible for the assembly of its core structure. Several other genes encoding the amino acid-derived building blocks, resistant proteins and tailoring steps are proposed but not characterized. As shown in the previous chapter, the azabicycle fragment of azinomycin B contains the bioactive aziridine group. My research focused on characterizing the proteins involved in the formation of the azabicycle moiety because understanding its biosynthetic origin will provide possible strategies to enhance the stability and bioactivity of azinomycin B for future drug development.

$^{13}$-C labeled feeding studies performed by former Watanabe group members had identified a few potential amino acid precursors to the azabicycle system.[35-36,51-52] The scrambling incorporation of labeled [1-$^{13}$C], [2-$^{13}$C] and [1,2-$^{13}$C] acetates at the C6-C7 and C12-C13 positions of azinomycin B suggests the contribution of a α-ketoglutarate. Possible precursors to α-ketoglutarate include proline, arginine, glutamine and glutamate, which would give raise to the azabicycle structure.[51] Knocking out *aziC2* and feeding the disruptant fermentation culture with potential isotopically labeled amino

acids had narrowed down the choice of precursors to L-glutamate. This chapter discusses the discovery of an unusual protein AziW, which mediates L-glutamate in the azabicycle formation.

## RESULTS AND DISCUSSION

### Bioinformatics Analysis and Previous Studies

*aziW* is located upstream of *aziC4* and it is not annotated in the published azinomycin B gene cluster. AziW is homologous (50% sequence identity) to the bacterial protein LysW (Figure 11). LysW has been shown to play a role during lysine biosynthesis in *Thermus thermophilus*. It contains a globular domain and a conserved C-terminal amino acid sequence EDWGE. The γ-carboxyl group of the C-terminal glutamate of LysW conjugates and modifies the amino group of α-aminoadipic acid (AAA). The LysW-AAA conjugation is activated by the protein LysX, an ATP-dependent ligase/acetyltransferase, through ATP phosphorylation. In addition, LysW also acts as a carrier protein in which its globular domain interacts electrostatically with other enzymes and mediates the formation of lysine (Figure 12).[53]

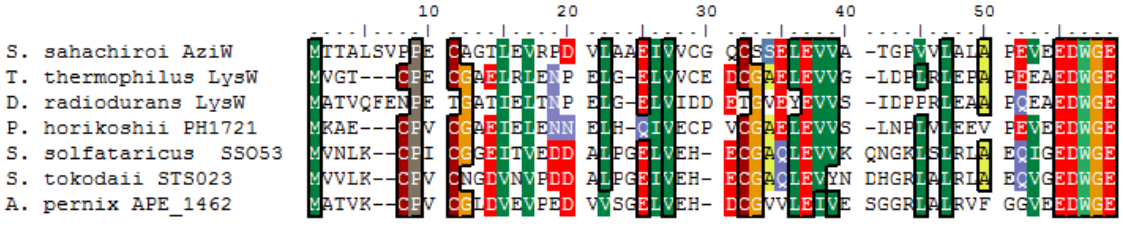


**Figure 11** Amino acid sequence alignment of LysW homologs from different species.

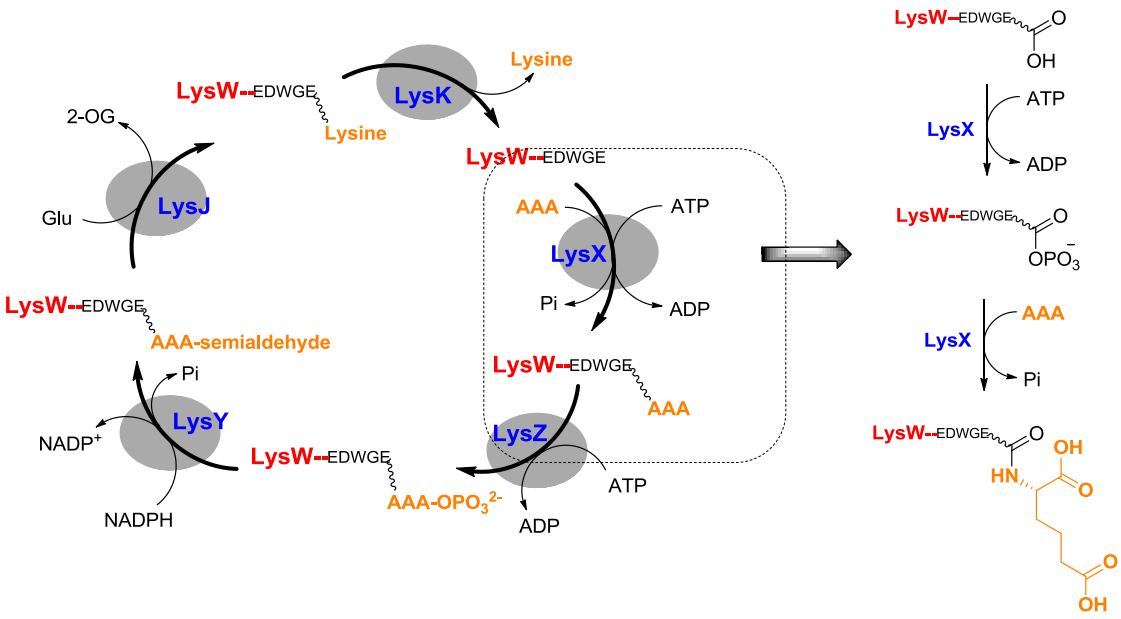


**Figure 12** The proposed functional roles of LysW in lysine biosynthesis of *Thermus thermophiles.* LysW acts as a protein carrier (Left) and ATP-dependent ligase (Right).

The amino acid sequence alignment of AziC2 (*Streptomyces sahachiroi*) and LysX (*Thermus thermophilus*) showed significant sequence identity (44%). The conserved regions that are important for LysW-LysX interaction in *Thermus thermophilus* are also present in AziC2. According to the protein BLAST, AziC2 has some similarities to the ATP-grasp superfamily. Enzyme in this family catalyzes the ligation of the carboxylate group and the amine/thiol group of two different molecules using ATP. Some examples are D-alanine-D-alanine ligase, glutathione synthetase, and ribosomal S6 modification enzyme RimK (Appendix Figure I). Based on this information, we proposed a similar pathway in which AziC2 activates the ligation of AziW and *L*-glutamate using ATP (Figure 13). The putative lysine biosynthetic gene cluster of all microorganisms that synthesizes lysine through a similar pathway has the

*lysW* located right next to the *lysX*. In case of *aziW*, it is very distant from *aziC2* in the azinomycin B gene cluster (Appendix Figure II).

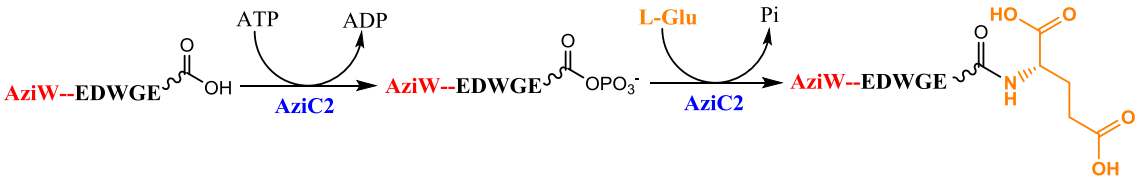


**Figure 13** The proposed function of AziW and AziC2.

Previous isotope-feeding experiments had identified L-glutamate as the precursor responsible for the assembly of the azabicycle moiety of azinomycin B. According to the *in vitro* studies performed by Dinesh Simkhada (Former post-doctoral, Watanabe group), AziC2 acts as an N-acetyltransferase. It catalyzes the formation of N-acetyl-L-glutamate using acetyl-CoA and L-glutamate. HPLC analysis of *in vivo* gene knockout of *aziC2* completely halted the azinomycin B production. However, feeding the mutant strain fermentation media with N-acetyl-L-glutamate did not restore the azinomycin B production as expected (unpublished data). This result led us to suspect whether acetyl-CoA is the original substrate for AziC2. Literature review revealed the presence of a small gene *aziW* in the azinomycin B gene cluster. Being a homolog to the LysW of *Thermus thermophilus*, we investigated the role of AziW.

A similar gene knockout study of *aziW* performed by Hillary Agbo (PhD, Watanabe group) showed no effect in azinomycin B production. However, disruption of *aziW* reduced the transcription level of the genes downstream of it (unpublished data).

To examine whether AziW or acetyl-CoA is the original substrate and to understand the role of AziW in the azabicycle biosynthesis, *in vitro* analysis of AziW with AziC2 were carried out.

**Inorganic Phosphate Detection by Malachite Green Assay**

*aziW* and *aziC2* were amplified from the genomic DNA of *S. sahachiroi* and introduced into the vector pET24b for protein overexpression. The inserts were verified by DNA sequencing reaction. *aziW*-pET24b and *aziC2*-pET24a were expressed in the *E. coli* BL21(DE3) strain via IPTG induction. The proteins were purified using His-Trap columns, confirmed by SDS-PAGE gel, and concentrated prior to *in vitro* assays.

Assuming AziC2 is a phosphatase, inorganic free phosphate would be released during the enzymatic reaction. Initial experiment was to monitor the release of free phosphate using malachite green assay kit (Cayman Chemicals). The complex formed between inorganic phosphate and malachite green molybdate under acidic condition can be measured spectrophotometrically at 620 nm. By comparing to the phosphate standards, we estimated the concentration of free phosphate being released in the reaction.

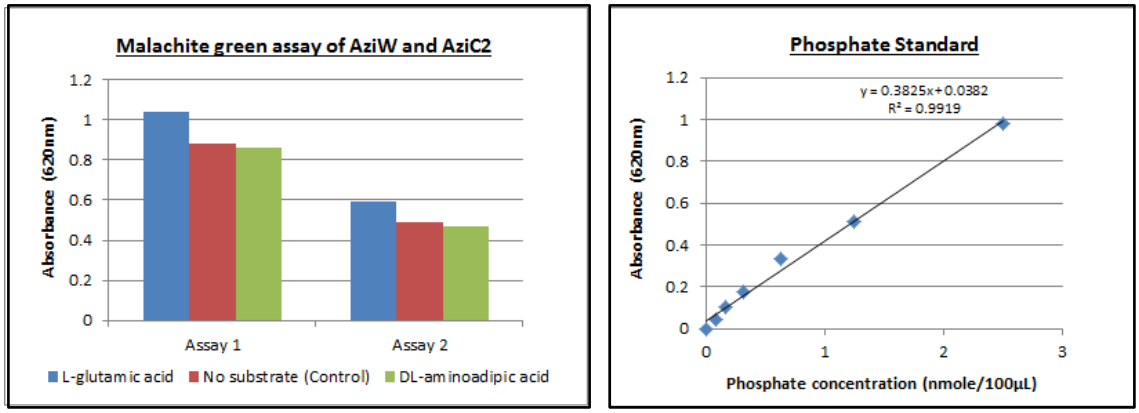


**Figure 14** Malachite green assay of AziC2 and AziW.

This result showed the release of approximately 0.5 nmole free phosphate per 100 µL of reaction mixture. In addition, it confirmed L-glutamate is the substrate rather tahn DL-2-aminoadipic acid as no free phosphate was detected compare to the control (Figure 14).

**Radioactive Labeling Assays**

To further understand how the inorganic phosphates were produced, we replaced ATP with [γ-$^{32}$P]-ATP in the reaction. Reactions containing purified protein(s) AziW and AziC2, [γ-$^{32}$P]-ATP and/or L-glutamate were set up. The proteins were loaded into a 15% SDS-PAGE gel after the reaction. The image of the gel was visualized using autoradiography (Figure 15).

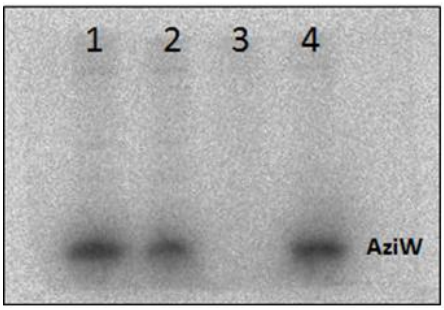


| Lane | 2mg/mL AziC2 | 2mg/mL AziW | 0.1mCi/mL [γ-$^{32}$P]-ATP | 5mM L-Glu | 1mM $MgSO_4$ |
|---|---|---|---|---|---|
| 1 | + | + | + | - | + |
| 2 | + | + | + | + | + |
| 3 | + | - | + | + | + |
| 4 | - | + | + | + | + |

**Figure 15** Result of [γ-$^{32}$P]-ATP study. 15% SDS-PAGE gel (left) and reaction conditions (right).

The dark bands shown on the gel image are [$^{32}$P] labeled AziW according to the distance the protein traveled on the SDS-PAGE gel. AziW in Lane#1 is [$^{32}$P] labeled; AziW in Lane#2 is also [$^{32}$P] labeled but at a lower concentration. In the absence of L-glutamate, AziW is expected to be labeled by [$^{32}$P]. The presence of L-glutamate, however, may or may not result in [$^{32}$P] labeled AziW depending on the substrates' ratio and if the reaction had gone to completion. In a control setup (Lane 3) where no AziW is added in the reaction mixture, no band is observed on the gel. Surprisingly, in another control setup (Lane 4) where no AziC2 was added, AziW is still being [$^{32}$P] labeled. This suggests the possibility of AziW self-activation in the phosphorylating process and that AziC2 may only involve in the transfer of L-glutamate to AziW.

To determine the role of AziC2, a similar experiment was performed using L-[$^{14}$C(U)]-glutamate in place of the L-glutamate. Reactions containing purified AziW and AziC2, L-[$^{14}$C(U)]-glutamate, and ATP were used. The image of the SDS-PAGE gel is shown below (Figure 16).


| Lane | 2mg/mL AziC2 | 2mg/mL AziW | 0.02mCi/mL L-[$^{14}$C]-Glu | 5mM ATP | 1mM $MgSO_4$ |
|---|---|---|---|---|---|
| 1 | + | + | + | + | + |
| 2 | + | - | + | + | + |
| 3 | - | + | + | + | + |
| 4 | + | + | 0.01mCi/mL | + | + |

**Figure 16** Result of [$^{14}$C]-glutamate study. 15% SDS-PAGE gel (left) and reaction conditions (right).

Due to the low-level radioactivity of [$^{14}$C], a faint band representing labeled AziW (Lane 1) showed up on the gel after prolonged exposure. This result is consistent with our prediction in which AziC2 only acts as a transferase. AziW is [$^{14}$C] labeled in the presence of AziC2 but not in the absence of it. No band is observed in the controls (Lane 2 and Lane 3). The band in Lane 4 was not observed due to low intensity. This result supports the hypothesis that phosphorylation of AziW is self-activated and the ligation of L-glutamate afterward is done by AziC2.

**SIGNIFICANCE**

AziW has been shown to take part in the reaction under the assayed conditions. Inorganic phosphates were detected in the malachite green assay which indicates the consumption of ATP during the reaction. [$\gamma$-$^{32}$P]-ATP radioactive labeling study clearly showed the incorporation of [$^{32}$P] in AziW. Since the proteins were heat denatured prior to loading into the SDS-PAGE gel, a bond is formed between the C-terminal carboxylic group of AziW and [$^{32}$-P]. The result of the L-[$^{14}$C(U)]-glutamate labeling experiment though promising has the necessity to repeat it using signal intensifier. Unlike the LysW

and LysX of *Thermus thermophilus*, AziW appears to be phosphorylated via self-activation and AziC2 serves only as a transferase in our case.

The preliminary results for characterizing AziW support our hypothesis so far. Future plan is to detect the L-glutamate linked-AziW intermediate using protein mass spectrometry. We will also attempt to differentiate the bands for AziW and L-glutamate linked-AziW in the reaction mixture using a higher resolution 12% Tricine-SDS-PAGE protein gel (resolution <2kDa) and analyze them using protein mass spectrometry. In addition, we can validate the reaction site, the C-terminal glutamate, of AziW via *in vitro* analysis with AziC2 using mutant AziW containing different amino acid, such as glutamine, alanine, valine or leucine, in place of the C-terminal glutamate. A custom-made AziW with an additional L-glutamate in its C-terminal may be used to feed into the AziC2 disruptant fermentation broth follow by HPLC analysis of azinomycin B production.

## EXPERIMENTAL PROCEDURES

### Instrumentation and General Methods

All primers used for DNA amplifications were ordered through Gene Technologies Lab (GTL) at Texas A&M University. DNA sequencing was also performed by GTL. All chemicals were purchased from Sigma-Aldrich. Malachite green phosphate assay kit was purchased from the Cayman Chemical. Radioactive labeled compounds were obtained from Perkin Elmer. Inorganic phosphate concentrations were determined in a 96-well plate using BioTek FL800 fluorescence microplate reader. Protein concentrations were analyzed via Bradford method (Standard: Bovine serum

albumin with linear range of 0.5 mg/mL to 5 mg/mL). Autoradiograph is developed using Fuji X-ray film developer. Primers, plasmids and strains used in this study are listed in Table 1. The map of the plasmid constructs is presented in Appendix Figure 4.

**Table 1** Primers, plasmids and strains used in the AziC2 and AziW studies.

| **Primer/ plasmid/ strain** | **Description** | **Source** |
|---|---|---|
| **Primers** | | |
| *lysW*_EcoRI _F | GAATTCATGCACCACCACCACCACCACACTA CGGCGCTGAGCGTGC | This study |
| *lysW*_HindIII_R | AAGCTTCTACTCGCCCCAGTCCTCTTCG | This study |
| **Plasmids** | | |
| pET-24a | T7 expression vector, C-terminal $His_6$-Tag, Kanamycin resistance | Novagen |
| pET-24b | T7 expression vector, C-terminal $His_6$-Tag, Kanamycin resistance | Novagen |
| pET24a-*aziC2* | *aziC2* gene (861 bp) was inserted at *BamH*I and *Hind*III sites | Dinesh Simkahda |
| pET24b-*aziW* | *aziW* gene (180 bp) was inserted at *Eco*RI and *Hind*III sites | This study |
| **Strains** | | |
| *S. sahachiroi* | Azinomycin B producing strain, wild type | ATCC |
| *E. coli* DH10B | Cloning host | Invitrogen |
| *E. coli* BL21(DE3) | Protein expression host | Invitrogen |

**Cloning, Protein Overexpression, and Purification of AziC2**

*aziC2* was cloned in vector pET-24a with *BamH*I/ *Hind*III site. The construct pET24a-*aziC2* was transformed in BL21(DE3) *E. coli* strain for protein overexpression. A 5 mL overnight culture in LB media containing 50 µg/mL kanamycin was added to 1L media and grown till an $OD_{600}$ of 0.8. The culture was induced with 1 mM IPTG and

incubated at 16 °C for 22-24 hours prior to harvest. The cells were centrifuged at 6,000×g for 20 min, washed twice with cold 20 mM Tris-HCl buffer (300 mM NaCl and 10% glycerol at pH 8) and re-suspended in the same buffer containing 1 mM dithiothreitol (DTT) and 1 mM phenyl methylsulfunyl fluoride (PMSF). The cell pellets were sonicated on ice water bath using Branson Sonifier 450 (Branson Ultrasonics) fitted with a micro tip, output setting 6, duty cycle 50%, for 8 cycles for 30 sec each and centrifuged for 1 h at 12,000×g.

The soluble protein was purified by Nickel affinity chromatography, His Trap ™ FF 5 ml column (GE Healthcare Life Sciences), according to the instructions provided by the supplier (Appendix Figure 3). The purified fractions eluted at 100mM imidazole buffer were desalted and concentrated to 2 mg/mL using Amicon® 10K Ultra centrifugal filter (EMD Millipore).

**Cloning, Protein Overexpression, and Purification of AziW**

*aziW* was cloned in vector pET-24b with N-terminal $His_6$-Tag and *EcoR*I/ *Hind*III site. The construct pET24b-*aziW* was transformed in BL21(DE3) *E. coli* strain for protein overexpression. A 5 mL overnight culture in LB media containing 50 µg/mL kanamycin was added to 1L media and grown till an $OD_{600}$ of 0.8. The culture was induced with 1 mM IPTG and incubated at 16 °C for 24 hours prior to harvest. The cells were centrifuged at 6,000×g for 20 min, washed twice with cold 20 mM Tris-HCl buffer (300 mM NaCl and 10% glycerol at pH 8) and re-suspended in the same buffer containing 1 mM dithiothreitol (DTT) and 1 mM phenyl methylsulfunyl fluoride (PMSF). The cell pellets were sonicated on ice water bath using Branson Sonifier 450

(Branson Ultrasonics) fitted with a micro tip, output setting 6, duty cycle 50%, for 8 cycles for 30 sec each and centrifuged for 1 h at 12,000×g.

The soluble protein was purified by Nickel affinity chromatography, His Trap ™ FF 5 ml column (GE Healthcare Life Sciences), according to the instructions provided by the supplier. The purified fractions eluted at 100mM imidazole buffer were desalted and concentrated to 2 mg/mL using Amicon® 10K Ultra centrifugal filter (EMD Millipore). To better visualize the protein size on SDS-PAGE, further purification was performed on selected fractions. Purified protein fractions were cleaned up by passing through Q-sepharose column (Sigma-Aldrich) and eluted with different concentration of NaCl buffer (0.10M, 0.25M, 0.50M and 0.75M NaCl). Each fraction was analyzed by 15% SPS-PAGE.

***In vitro* Malachite Green Assay**

A reaction mixture containing 0.75 mg purified AziW, 1 mg purified AziC2, 1 mM $MgSO_4$, 5 mM L-glutamate or DL-2-aminoadipic acid and 5 mM ATP in 100 mM HEPES at pH 8 was incubated at 37°C for 30 minutes in a 96-well plate. The reaction was terminated by adding an equal volume of 10 mM EDTA (pH 8). The malachite green solutions were added to the samples according to the protocol provided in the Malachite Green Phosphate Assay Kit (Cayman Chemical). The absorbance of the phosphate standards ranging from 1.56 μM to 25 μM (in duplicate) and the samples (in triplicate) were measured at 620 nm using BioTek FL800 fluorescence microplate reader.

**Phosphotransferase Activity of AziW using [$^{32}$P]-ATP**

A reaction mixture containing 2 mg of purified AziW, 2 mg of purified AziC2, 5 mM N-acetyl-L-glutamate, 1 mM $MgSO_4$, 0.1 mCi/mL [$\gamma$-$^{32}$P]-ATP in 100 mM HEPES buffer at pH 8 was incubated at room temperature for 1 hour. The reaction mixture was filtered using Amicon® 3K Ultra centrifugal filter. The proteins were loaded into a 15% SDS-PAGE gel. After electrophoresis, the gel was washed with buffer containing 5% trichloroacetic acid (TCA) and 1% sodium pyrophosphate (NaPPi). The image of the gel was visualized using autoradiography.

**L-[$^{14}$C(U)]-glutamate Labeling Assay of AziW**

A reaction mixture containing 2 mg of purified AziW, 2 mg of purified AziC2, 0.02 mCi/mL L-[$^{14}$C(U)]-glutamate, 1 mM $MgSO_4$, 5 mM ATP in 100 mM HEPES buffer at pH 8 was incubated at room temperature for 3 hours. The reaction mixture was filtered using Amicon® 3K Ultra centrifugal filter. The proteins were loaded into a 15% SDS-PAGE gel. After electrophoresis, the gel was washed with buffer containing 5% trichloroacetic acid (TCA) and 1% sodium pyrophosphate (NaPPi). The image of the gel was visualized using autoradiography.

# CHAPTER III

## EXPLORING THE AZABICYCLE BIOSYNTHETIC PATHWAY OF AZINOMYCIN B

### INTRODUCTION

The biosynthetic pathway of the azabicycle of azinomycin B is proposed based on literature studies and protein BLAST analysis. Putative substrates and cofactors of the corresponding enzymatic reaction are detailed in Figure 17 (Watanabe group). *aziC3*, *aziC4*, *aziC5* and *aziC6* genes are involved in the first portion of the proposed biosynthetic route to the azabicycle moiety. AziC3 and AziC4 are homology to N-acetylglutamate kinase and N-acetyl-γ-glutamyl-phosphate reductase of lysine biosynthesis while AziC5 and AziC6 are homology to N-terminal transketolase and C-terminal transketolase of ornithine biosynthesis respectively (Table 2).[32] N-acetyl-*L*-glutamate is converted into the dihydroxyketone intermediate in four steps. N-acetylglutamate kinase (AziC3) catalyzes the phosphorylation of the γ-carboxyl group of N-acetyl-*L*-glutamate (a promising substrate for AziC3) using ATP. The phosphorylated intermediate converts into a semialdehyde by N-acetyl-γ-glutamyl-phosphate reductase (AziC4) and NAD(P)H. The transketolase subunit AziC5 and AziC6 catalyze the transfer of two carbons unit from β-hydroxypyruvic acid (HPA) to the semialdehyde using thiamine pyrophosphate (TPP) and magnesium (II) ion as cofactors.

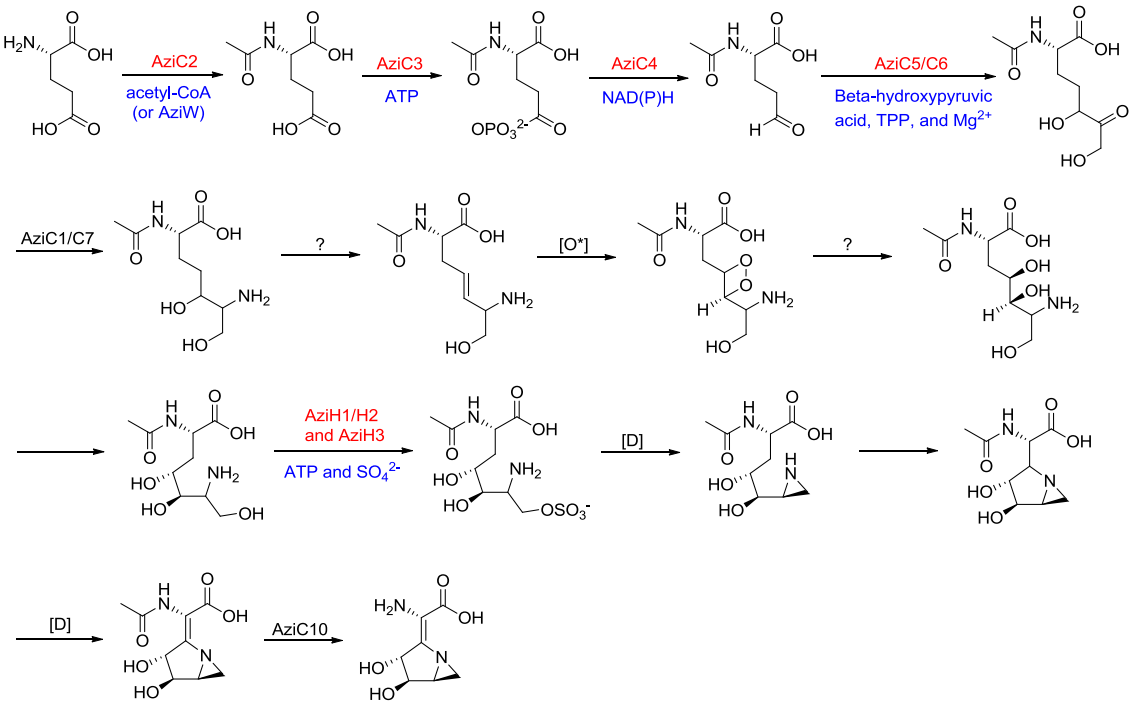


**Figure 17** The proposed biosynthetic route to the azabicycle.

Previous *in vivo* gene knockout studies of *aziC2* performed by Dinesh Simkhada (unpublished data) ceased the production of azinomycin B in *Streptomyces sahachiroi*, which indicated the importance of AziC2 in the azinomycin B formation. Based on this result, we continued to explore the function of enzymes subsequent to AziC2 that may involve in the azabicycle formation. This chapter details experiments performed in verifying the proposed function of each enzyme via both *in vitro* and *in vivo* studies.

**Table 2** The proposed function of AziC3, AziC4, AziC5 and AziC6.

| Gene | Proposed function | Organism | Similarity/ Identity (%) |
|---|---|---|---|
| *aziC3* | N-acetylglutamate kinase | *Thermus thermophilus* | 55/36 |
| *aziC4* | N-acetyl-γ-glutamyl-phosphate reductase | *Deinococcus geothermalis* | 55/45 |
| *aziC5* | N-terminal transketolase | *Thermotoga maritima* | 61/44 |
| *aziC6* | C-terminal transketolase | *Clostridium perfringens* | 61/41 |

## RESULTS AND DISCUSSION

### Protein Overexpression of AziC3, AziC4, AziC5 and AziC6

*aziC3*, *aziC4*, *aziC5* and *aziC6* genes were individually cloned in the expression vector pET24b and expressed in *Escherichia coli* BL21(DE3) strain for *in vitro* assays. All proteins were expressed in the soluble form except AziC4, which finally became soluble when it was cloned in pET21a (ampicillin resistance) and co-expressed with AziC3 (Figure 18).

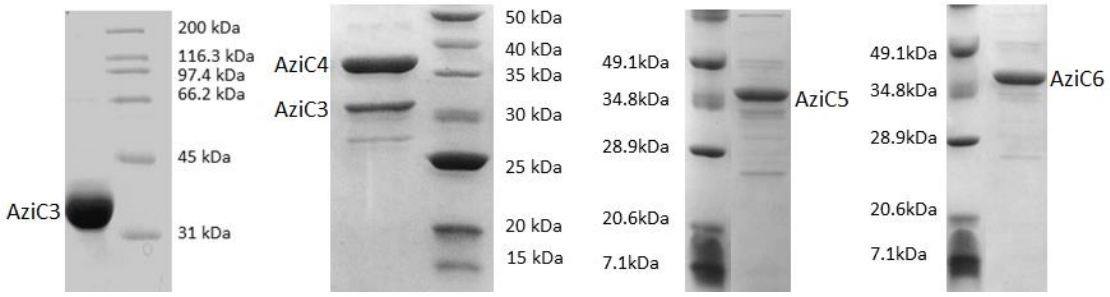


**Figure 18** SDS-PAGE gels showing purified AziC3, AziC4, AziC5 and AziC6.

## Hydroxamate-$Fe^{3+}$ Complex Colorimetric Assay

Initial experiment to determine the *in vitro* activity of AziC3 is to identify the phosphorylated product. AziC3 catalyzes the conversion of N-acetyl-*L*-glutamate to N-acetyl-*L*-glutamate phosphate intermediate, which is too unstable to be detected using mass spectrometry. To overcome the difficulty in trapping unstable intermediate, we used hydroxylamine hydrochloride ($NH_2OH{\cdot}HCl$) to convert the phosphate intermediate formed into N-acetyl-L-glutamyl-γ-hydroxamate. The N-acetyl-L-glutamyl-γ-hydroxamate in turn complexes with ferric chloride ($FeCl_3$) at which the absorbance can be measured spectrophotometrically (Figure 19).[54]

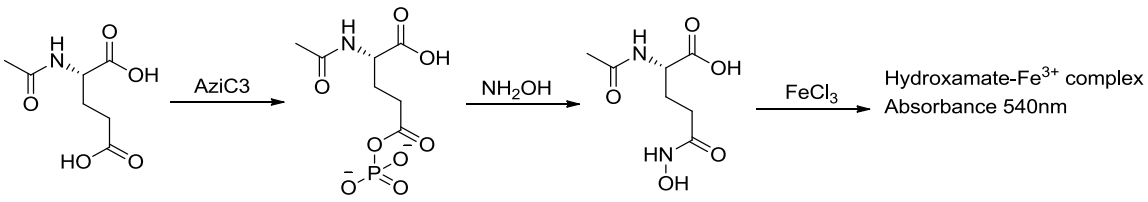


**Figure 19** The formation of hydroxamate-$Fe^{3+}$ complex by AziC3.

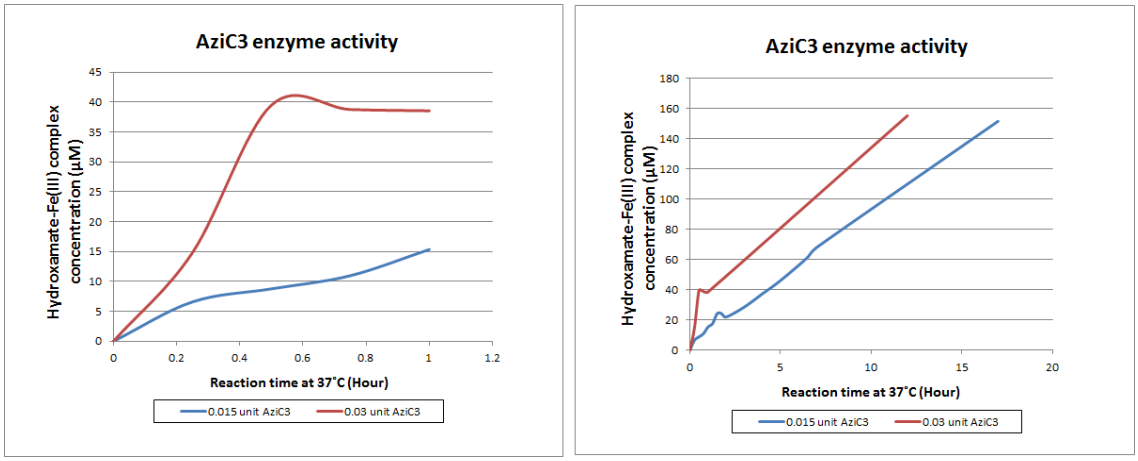


**Figure 20** Result of hydroxylamine assay by AziC3.

One unit of AziC3 is defined as the amount of enzyme catalyzed the formation of 1μmole of N-acetyl-L-glutamyl-γ-hydroxamate-$Fe^{3+}$ complex per minute under the assay conditions. The molar absorption coefficient **ε** of this complex at 540nm is 0.5188 $M^{-1}cm^{-1}$. Based on this information, the concentration of N-acetyl-L-glutamyl-γ-hydroxamate-$Fe^{3+}$ complex in μM was calculated (A = **ε**lc) and plotted against the reaction time at 37°C (Figure 20). This result primarily confirmed the activity of AziC3.

**[γ-$^{32}$P]-ATP Labeling Assay**

To further characterize the phosphorylated intermediate, [γ-$^{32}$P]-ATP was used to label the carboxylic group of N-acetyl-*L*-glutamate during the AziC3 enzymatic reaction. A reaction containing AziC3, N-acetyl-L-glutamate, and [γ-$^{32}$P]-ATP was set up. After the reaction, the protein was removed and the reaction mixture was spotted on a reverse phase TLC plate. The TLC plate was developed using chloroform/butanol mixture and visualized using autoradiography. Unreacted [γ-$^{32}$P]-ATP is polar and did not move on the TLC plate. The [γ-$^{32}$P] labeled product N-acetyl-L-glutamate phosphate is comparably less polar and traveled up the TLC plate as shown in Figure 21. This experiment identified the phosphorylated intermediate which is in consistent with the initial experiment.

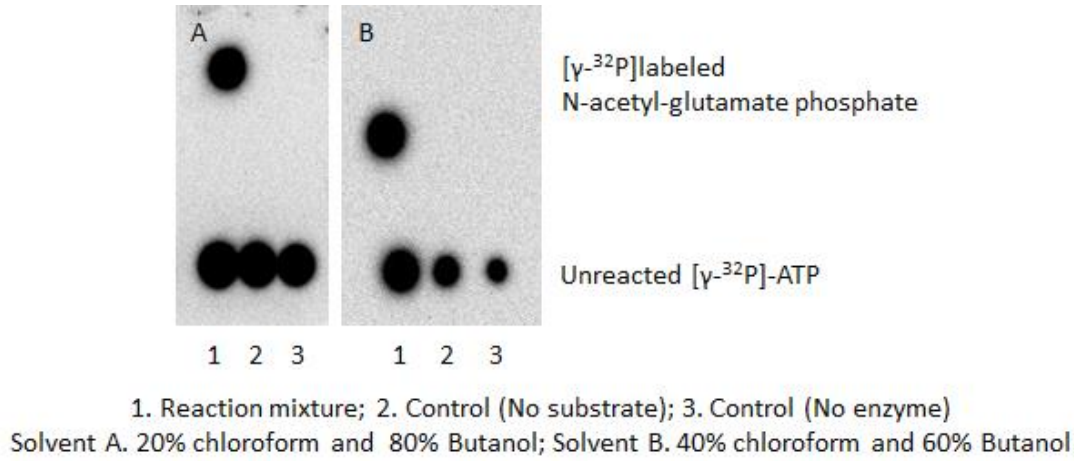


**Figure 21** Image of reverse phase TLC plate of AziC3 [γ-$^{32}$P]-ATP labeling study.

## Synthesis of Substrate Analog: N-acetyl-glutamate Cysteamine

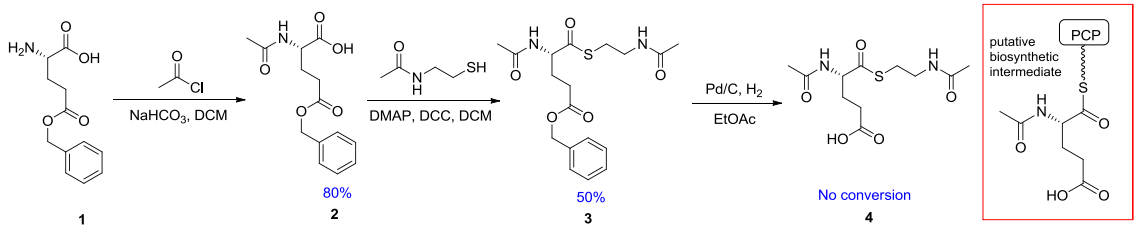


**Scheme 1** Proposed synthetic route to N-acetyl-glutamate cysteamine.

To better mimic the putative biosynthetic intermediate for AziC3 enzymatic reaction, we attempted to synthesize the peptidyl carrier protein (PCP)-linked N-acetyl-L-glutamate. The synthetic strategy is outlined in Scheme 1. Acetylation of glutamate-γ-benzyl ester **1** generated the acetylated product **2** (Appendix Figure 5).[55] Hydrolysis of the unprotected carboxylic group with N-acetyl-cysteamine yielded the cysteamine-linked acetyl-glutamate-γ-benzyl ester **3** (Appendix Figure 6).[56] Deprotection of benzyl ester group to give the desired final product **4**.[55] Unfortunately, we are unable to remove

the benzyl ester group in the final step due to poisoning of catalyst used for hydrogenation. Palladium and platinum was used as the catalyst with increased reaction pressure, however no conversion occurred.

**Gene Knockout and Complementation Study of AziC3**

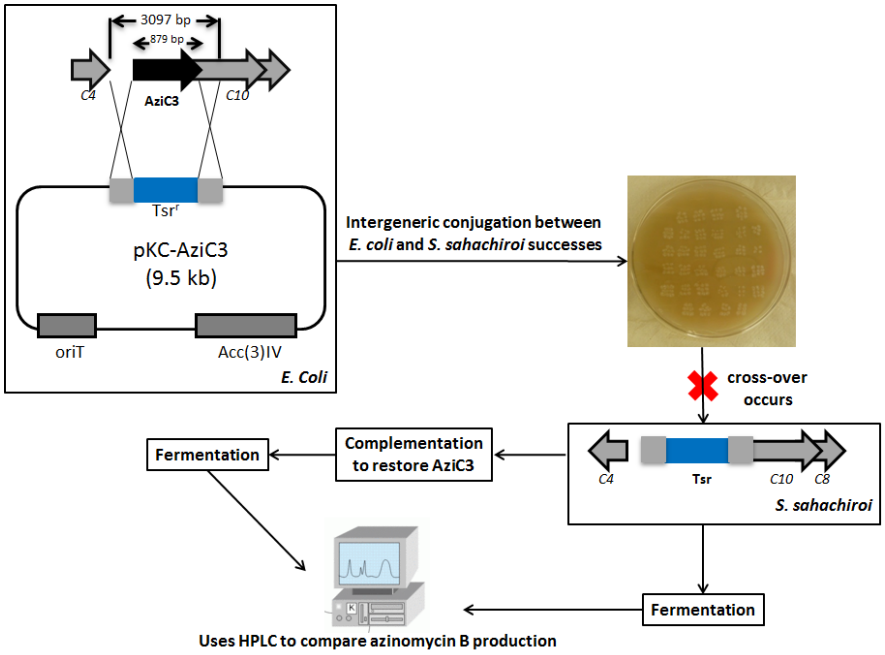


**Figure 22** An outline of the *in vivo* analysis of AziC3.

*In vitro* characterization of proteins function may not completely prove their involvement in the azinomycin B biosynthesis. To better understand their role in the original strain (*Streptomyces sahachiroi*), gene knockout study is usually performed in parallel. *aziC3* gene disruption was carried out. Thiostrepton (*tsr*) resistance gene and the upstream and downstream regions of *aziC3* were cloned into the *E. coli-Streptomyces* shuttle vector pKC1139 (aparamycin resistance). Intergeneric conjugation

was performed between the plasmid in *E. coli* S-17 strain and *Streptomyces sahachiroi* wild-type spore. The wild-type *Streptomyces sahachiroi* will become resistant to both aparamycin and thiostrepton upon successful conjugation. After several generations, gene crossover should occur and the mutant strain would become thiostrepton resistance and sensitive to aparamycin. In our case, the conjugal transformation was successful; however no cross-over had occurred after $30^{th}$ generations. We are unable to explain the circumstance and have been working on the conjugation steps. Figure 22 detailed the entire process of gene disruption and complementation. The azinomycin B production of the restored and mutant strain will finally be analyzed by using HPLC.

**Kinetic Measurement of AziC3 and AziC4 Coupling Reaction**

Characterization of AziC4 is assayed in conjunction with AziC3 due to the instability of phosphate intermediate as its substrate. The activity of AziC4 was determined by a coupled reaction with AziC3. AziC4 catalyzes the formation of N-acetyl-*L*-glutamate semialdehyde from a very unstable substrate N-acetyl-*L*-glutamate phosphate using NAD(P)H. In the coupling reaction, N-acetyl-*L*-glutamate was first converted into N-acetyl-*L*-glutamate phosphate by AziC3 and then further reduced to N-acetyl-*L*-glutamate semialdehyde by AziC4 while NAD(P)H was oxidized to $NAD(P)^+$. The rate of NAD(P)H oxidation was monitored as a change in absorbance at 340nm using UV-vis spectrophotometer (Figure 23).[57] The rate of $NAD(P)^+$ formation is equal to the rate of product formation. The kinetic data is reported in Table 3.

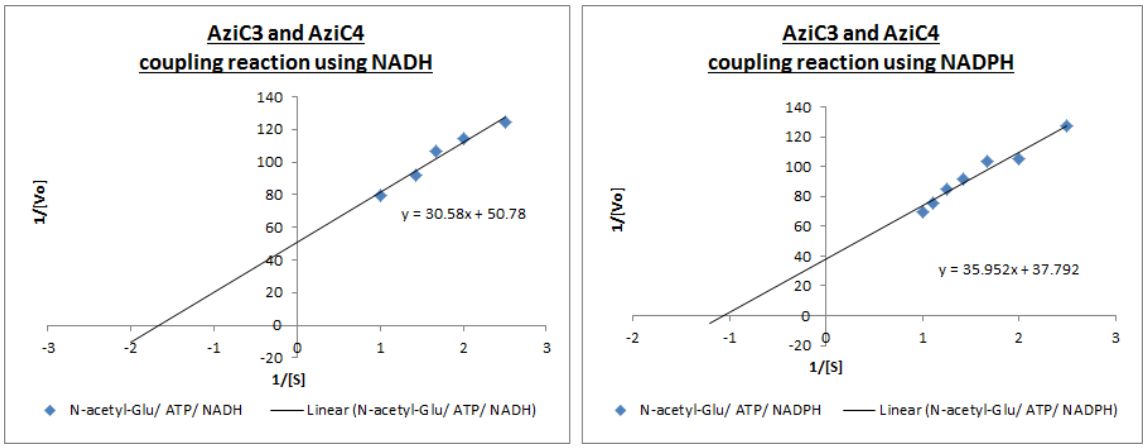


**Figure 23** Result of AziC3 and AziC4 coupling assay. NADH (left) and NADPH (right).

**Table 3** Kinetic data of AziC3 and AziC4 coupling assay.

| **Kinetic data** | **N-acetyl-Glu/ ATP/ NADH** | **N-acetyl-Glu/ ATP/ NADPH** |
|---|---|---|
| [AziC4] | 4.13 uM | 4.13 uM |
| Vmax | 0.02105 mM/min | 0.03084 mM/min |
| Km | 0.6859 $mM^{-1}$ | 1.2220 $mM^{-1}$ |
| Kcat/ Km | 5.098 $mM^{-1}min^{-1}$ | 7.468 $mM^{-1}min^{-1}$ |

AziC4 accepts both NADH and NADPH as a cofactor and did not show a significant preference to either one of them. Optimizing the reaction conditions may reveal the actual cofactor of this reaction and give us a more accurate kinetic result. Nonetheless, these data give us enough confident to move on to characterize AziC5 and AziC6 using the putative substrates.

## SIGNIFICANCE

Though these protein function is quite common in the biosynthesis of natural compounds, characterizing them are valuable for us to fully understand the biosynthesis of the azabicycle moiety. If the role of AziW in the azabicycle biosynthetic pathway is

confirmed, we will be able to repeat the *in vitro* assays performed with AziC3 and/or AziC4 by using AziW in place of acetyl-CoA. The substrate preference and the rate of reaction can be compared. Further experiments for AziC5, AziC6, and the enzymes involved in the rest of the azabicycle biosynthetic pathway will depend upon the success in synthesizing substrate analogs.

## EXPERIMENTAL PROCEDURES

### Instrumentation and General Methods

All primers used for DNA amplifications were ordered through Gene Technologies Lab (GTL) at Texas A&M University. DNA sequencing was also performed by GTL. All chemicals were purchased from Sigma-Aldrich. Kinetic data were measured using spectronic gensys spectrophotometer. Protein concentrations were analyzed via Bradford method (Standard: Bovine serum albumin with linear range of 0.5 mg/mL to 5 mg/mL). Radioactive labeled compounds were obtained from Perkin Elmer. Autoradiograph is developed using Fuji X-ray film developer. Primers, plasmids and strains used in this study are listed in Table 4. The map of the plasmid constructs is presented in Appendix Figure 7.

**Table 4** Primers, plasmids and strains used in the AziC3, AziC4, AziC5 and AziC6 studies.

| Primer/ plasmid/ strain | Description | Source |
|---|---|---|
| **Primers** | | |
| *aziC3_ EcoR*I_F | GCGAATTCATGGCGCAGGATCCGAGG | This study |
| *aziC3_ Hind*III_R | CCAAGCTTGCCATCTTCGGGCCTCTCC | This study |
| *aziC3*_UP_F | GCAAGCTTACACATGACTACGGCGCTG | This study |

**Table 4** Continued

| Primer/ plasmid/ strain | Description | Source |
|---|---|---|
| *aziC3*_UP_R | GCAGATCTCGCCACGTTCAGGCTCT | This study |
| *aziC3*_DN_F | GCTCTAGACGACCGGATGGCCGAG | This study |
| *aziC3*_DN_R | GCCTTAAGAGCGGTCGAGGAGGATCAG | This study |
| *aziC4_BamH*I_F | AGGATCCATGCATGCCCACCCCAAGCT | This study |
| *aziC4_Hind*III_R | GAAGCTTGGCGGGGTGCAGTCCGGT | This study |
| *aziC5_EcoR*I _F | AGAATTCATGAGCCGCCCGCCGCTC | This study |
| *aziC5_Hind*III_R | AAGCTTCGCCGTACCTCCCTGCACGG | This study |
| *aziC6_EcoR*I _F | GAATTCATGACGACGGCGCGCCCC | This study |
| *aziC6_Hind*III_R | AAAGCTTTCCCCTCATGGTTGGGCCGG | This study |
| **Plasmids** | | |
| pGEM-T easy | Sub-cloning vector, *E. coli* | Promega |
| pET-21a | T7 expression vector, C-terminal $His_6$-Tag, Ampicillin resistance | Novagen |
| pET-24b | T7 expression vector, C-terminal $His_6$-Tag, Kanamycin resistance | Novagen |
| pET24b-*aziC3* | *aziC3* gene (879 bp) was inserted at *EcoR*I and *Hind*III sites | This study |
| pET21a-*aziC4* | *aziC4* gene (924 bp) was inserted at *BamH*I and *Hind*III sites | This study |
| pET24b-*aziC5* | *aziC5* gene (936 bp) was inserted at *EcoR*I and *Hind*III sites | This study |
| pET24b-*aziC6* | *aziC6* gene (1023 bp) was inserted at *EcoR*I and *Hind*III sites | This study |
| pkC1139 | *E. coli-Streptomyces* shuttle vector, Aparamycin resistance | |
| pkC1139-*aziC3*_UP | Upstream region (1113 bp) of *aziC3* was inserted at *Hind*III and *Xba*I sites | This study |
| pkC1139-*aziC3*_DN | Downstream region (1105 bp) of *aziC3* was inserted at *Xba*I and *EcoR*I sites | This study |
| **Strains** | | |
| *S. sahachiroi* | Azinomycin B producing strain, wild type | ATCC |
| *S. lividans TK24* | Heterologous expression strain, wild type | ATCC |
| *E. coli* DH10B | Cloning host | Invitrogen |
| *E. coli* BL21(DE3) | Protein expression host | Invitrogen |
| *E. coli* S-17 | Intergeneric conjugation, donor strain | Invitrogen |

**Cloning, Protein Overexpression, and Purification of AziC3, AziC4, AziC5 and AziC6**

*aziC3*, *aziC5*, and *aziC6* were individually cloned in vector pET-24b. *aziC4* was cloned in vector pET-21a. The construct was transformed in BL21(DE3) *E. coli* strain for protein overexpression. A 5 mL overnight culture in LB media containing 50 µg/mL kanamycin (100 µg/mL ampicillin for pET21a-*aziC4*) was added to 1L media and grown till an $OD_{600}$ of 0.8. The culture was induced with 1 mM IPTG and incubated at 16 °C for 22-24 hours prior to harvest. The cells were centrifuged at 6,000×g for 20 min, washed twice with cold 50 mM phosphate buffer (300 mM NaCl and 10% glycerol at pH 7) and re-suspended in the same buffer containing 1 mM dithiothreitol (DTT) and 1 mM phenyl methylsulfunyl fluoride (PMSF). The cell pellets were sonicated on ice water bath using Branson Sonifier 450 (Branson Ultrasonics) fitted with a micro tip, output setting 6, duty cycle 50%, for 8 cycles for 30 sec each and centrifuged for 1 h at 12,000×g.

The soluble protein was purified by Nickel affinity chromatography, His Trap ™ FF 5 ml column (GE Healthcare Life Sciences), according to the instructions provided by the supplier. The purified fractions were desalted and concentrated using Amicon® 10K Ultra centrifugal filter (EMD Millipore).

**Heterologous Expression of AziC3**

A construct consisted of the upstream region (1113 bp) and downstream region (1105 bp) of *aziC3* and a thiostrepton (*tsr*) resistance gene was created in the *E. coli-Streptomyces* shuttle vector pKC1139 (aparamycin resistance) . The thiostrepton gene

was inserted in between the regions. The construct in *E. coli* S-17 donor strain was transformed into *S. sahachiroi* wild-type spore via intergeneric conjugation.

A 5 mL culture of *E. coli* S-17 containing the pKC1139-*aziC3* was grown to an $OD_{600}$ of 0.4 with 50 mg/mL aparamycin. The cells were pelleted, washed with LB and re-suspended in 200 µL of LB. *S. sahachiroi* wild-type spore was grown on MS agar plate ( 20 g/L soy flour, 20 g/L manitol, 20 g/L LB agar and 2.03 g/L $MgCl_2 \cdot H_2O$) at 30°C for 7-10 days. The spores were suspended in 6 mL 2XYT medium (16 g/L difco bacto trypton, 10 g/L difco bacto yeast extract, 5 g/L NaCl and 40 µL 5N NaOH), filtered and heat shocked at 70°C for 10 minutes to activate germination. The spores were incubated at 37°C for 3-5 hours with shaking. After incubation, it was washed with 2XYT and re-suspended in 500 µL of 2XYT. Equal volume of *E. coli* and *S. sahachiroi* cultures were mixed thoroughly and plated on MS agar plates. The plates were incubated at 30°C for 16-22 hours prior to overlay with 50 µg/mL aparamycin and 25 µg/mL nalidixic acid.

**[$^{32}$P]-ATP labeling study of AziC3**

A reaction mixture contained 0.5 mg/mL purified AziC3, 10mM N-acetyl-L-glutamate, 20mM $MgCl_2$, 0.2mCi/mL [$\gamma$-$^{32}$P]-ATP and 100mM potassium phosphate buffer at pH 7.5 was incubated at room temperature for 16 hours. The reaction mixture was filtered using Amicon® 10K Ultra centrifugal filter to remove the protein and the flow through was spotted on reverse phase TLC plate. The TLC plate was developed using chloroform/butanol mixture (1:4-V/V% or 2:3-V/V%) and visualized using autoradiography.

**Colorimetric Assay of AziC3**

A mixture consisted of 400 mM $NH_2OH{\cdot}HCl$, 400 mM Tris-HCl, 20 mM $MgCl_2$ and 10 mM ATP was first adjusted to pH 7.2 using NaOH. The mixture was transferred into a microcuvette. 0.5 mg/mL purified AziC3 was added. The reaction was started by adding 40 mM N-acetylglutamate (pH 7). After incubated at 37°C for a certain period of time (15 minutes to 1 hour/ overnight), the reaction was terminated by adding an equal volume of a solution containing 5% (w/v) $FeCl_3.6H_2O$, 8% (w/v) trichloroacetic acid, and 0.3 M HCl. The absorbance was measured at 540 nm spectronic gensys spectrophotometer.

**Synthesizing N-acetyl-glutamate Cysteamine**

1 equivalent (0.2 g) of glutamate-γ-benzyl ester, 1.5 equivalents (100 μL) of acetyl chloride and 2 equivalents (0.14 g) of $NaHCO_3$ in 5 mL DCM were stirred at room temperature for 24 hours. The reaction mixture was filtered and rotavapored to remove $NaHCO_3$ and DCM. The acetylated product was purified using column chromatography (2% methanol in chloroform).

1 equivalent (2 g) of the acetylated product, 1 equivalent (0.85 g) of N-acetylcysteamine and 1 equivalent (0.88 g) of dimethylaminopyridine (DMAP) in 25 mL DCM were stirred on ice/acetone bath for 15 minutes. 1 equivalent (1 g) of N, N′-dicyclohexylcarbodiimide (DCC) was added dropwise to the reaction mixture and it was stirred at room temperature for 20 hours. The reaction mixture was filtered through celite, washed with DCM, extracted with saturated $NaHCO_3$ and NaCl and dried using

$MgSO_4$. The cysteamine-linked product was purified using column chromatography (2% methanol in chloroform).

**Continuous reaction of AziC3 and AziC4**

A reaction mixture consisted of N-acetylglutamate (0.05 mM to 1 mM at pH 7), 10 mM ATP, 0.3 mM NAD(P)H, 20 mM $MgCl_2$ and 100 mM phosphate buffer (pH 7.2) was kept at 4°C in a microcuvette. 2 mg/mL of purified AziC3 and AziC4 protein mixture (co-expressed) was added to the mixture. The rate of decrease in the concentration of NAD(P)H was measured immediately at 340 nm using UV-vis spectrophotometer over a period of 180 seconds.

# CHAPTER IV

## MECHANISTIC STUDY OF THE ENZYMES INVOLVED IN SULFATION

### INTRODUCTION

Anti-tumor agents usually covalently bind to their targets through specific moieties in their structures. Common DNA alkylating groups of natural product are cyclopropane, epoxide, and aziridine rings. These highly strained three-membered ring systems cross-link with double-stranded DNA. Mitomycin C and dynemicin A are examples of three-membered ring containing drugs used in cancer treatment. The mode of action of mitomycin C (Figure 24) and dynemicin A (Figure 25) are depicted below. Mitomycin C is first activated by a two electrons quinone reduction to form a hydroquinone. The hydroquinone intermediate losses a methanol group, follows by a proton-assisted aziridine ring opening, and then alkylates DNA.[58] DNA cleavage by dynemicin A is induced by NAPDH. The activated dynemicin A cut the 3' side of purine bases at specific positions such as 5'-GT, 5'-GC and 5'-AG to cause DNA damage.[59] The biosynthesis of these compounds have been of research interest for many years. The understanding of how these unique ring structures are formed will provide valuable information in future drug development.

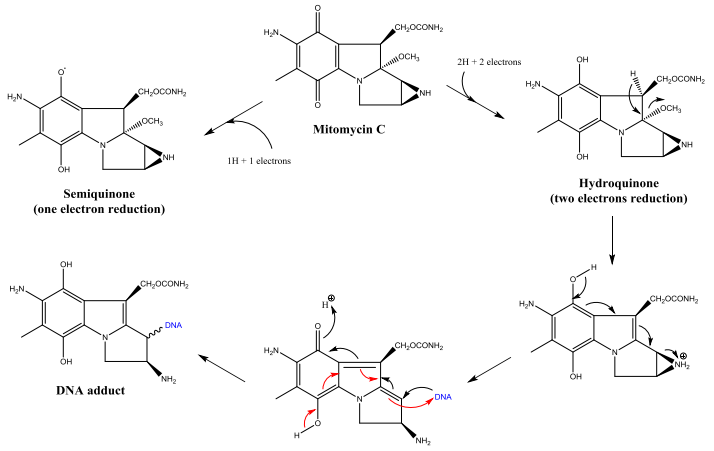


**Figure 24** The mode of action of mitomycin C: DNA cross-link. **Adapted from** Cummings *et al.* [58].

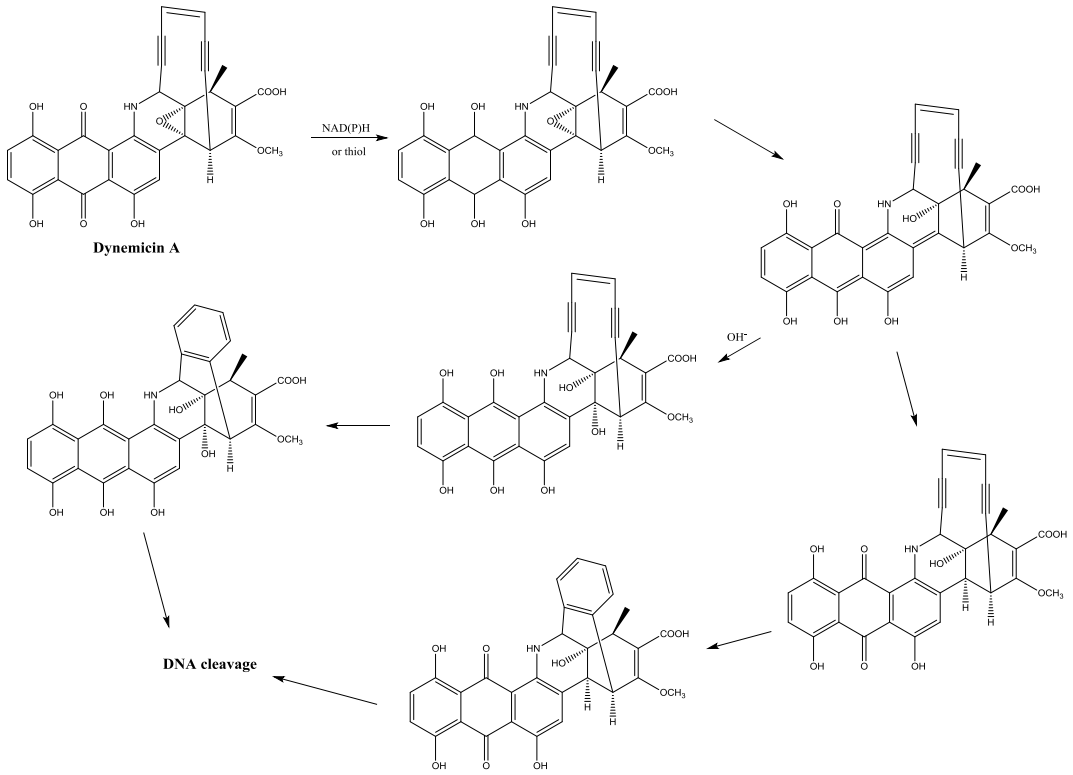


**Figure 25** The mode of action of dynemicin A: DNA cleavage. **Adapted from** Sugiura *et al.* [59].

Azinomycin B is one of the potent anti-tumor agents consists of the aziridine group under study. The mechanism of its aziridine ring formation is by far the most interesting part of the azabicycle moiety because very little is known about its biosynthesis. Out of all the aziridine-containing natural products identified, only three of them have their gene cluster published, which includes azinomycin, azicemicin, and mitomycin. A possible mechanism for the aziridine ring formation proposed by Bicker and Fischer is as follow: sulfotransferases convert the β-amino alcohol to sulfate ester intermediate using PAPS, which is formed by ATP and $SO_4^{2-}$ enzymatically, and subsequent ring closure gives the aziridine (Figure 10).[50] Based on this observation and sequence homology analysis (Table 5), we proposed a mechanistic scheme of the aziridine ring formation (Figure 26).

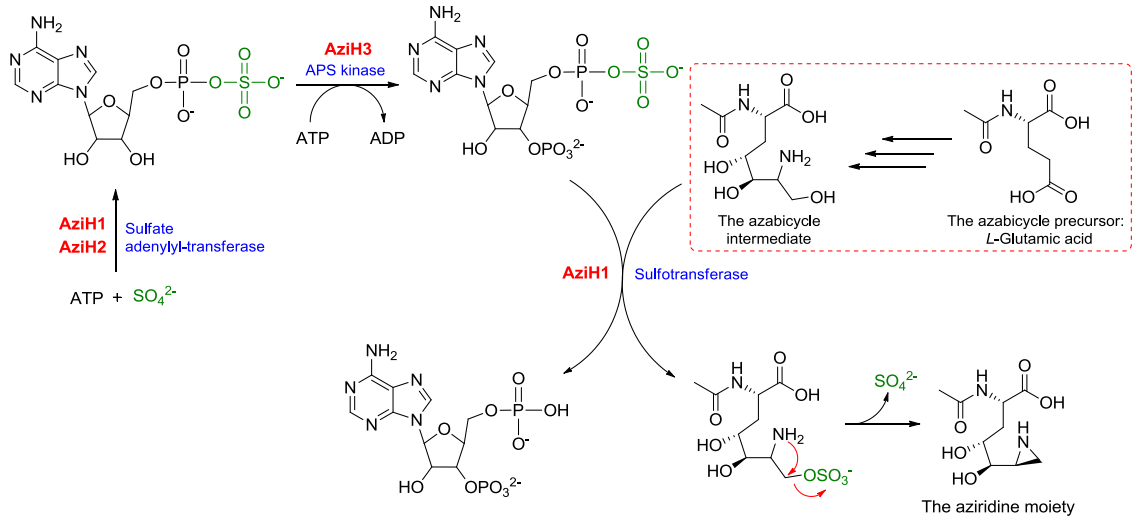


**Figure 26** The proposed mechanistic scheme of the aziridine ring formation.

**Table 5** The proposed function of AziH1, AziH2, and AziH3.

| Gene | Proposed function | Organism | Similarity/ Identity (%) |
|---|---|---|---|
| *aziH1* | Sulfate adenyltransferase subunit II or PAPS reductase/ PAPS sulfotransferase | *Escherichia coli* | 46/63 |
| *aziH2* | Sulfate adenyltransferase subunit I | *Escherichia coli* | 47/63 |
| *aziH3* | Adenylsulfate kinase/ APS kinase | *Escherichia coli* | 41/59 |

The *in vivo* gene knockout study of *aziH1* and *aziH2* (performed by Huitu Zhang) showed a decrease in azinomycin B production. The *in vitro* studies of the aziridine ring formation are currently in progress.

## RESULTS AND DISCUSSION

### Protein Overexpression of AziH1, AziH2 and AziH3

*aziH1*, *aziH2* and *aziH3* were individually cloned in the expression vector pET24b (kanamycin resistance) and expressed in *Escherichia coli* BL21 (DE3) strain. AziH3 was expressed as a soluble protein and purified using His-Trap column. AziH1 and AziH2 are not quite soluble and we are experiencing difficulties in the purification processes. Different cloning strategies and expression conditions were attempted; however, there were no improvement in protein solubility (Figure 27). The protein size of AziH3 shows up bigger on the SDS-PAGE gel but the actual size of AziH3 has been confirmed by MALDI-MS (Appendix Figure 8).

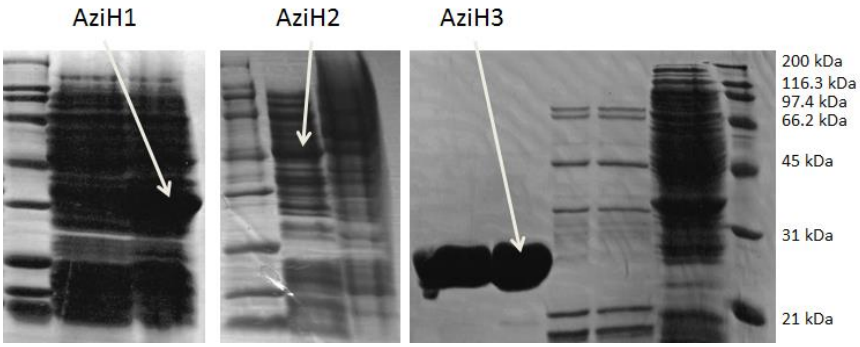


**Figure 27** SDS-PAGE of insoluble proteins AziH1 and AziH2 and purified AziH3.

## SIGNIFICANCE

One of the most challenging parts in enzymatic study is to obtain soluble, active and purified proteins. Protein solubility is a common problem when it is expressed in a foreign host. Strategies like modifying expression conditions, co-expressing with soluble protein or as a fusion protein and optimizing DNA codon usage to meet the host preference may solve the solubility problem. However, optimizing expression conditions and protein co-expression have failed with AziH1 and AziH2. Other practical approaches include expressing the proteins in *Streptomyces lividans*, synthesizing the genes with codon usage optimized for *E. coli*., purifying the proteins from inclusion body, or expressing them as a fusion protein. The last resort will be to perform the enzymatic studies using crude AziH1 and AziH2.

## EXPERIMENTAL PROCEDURES

### Instrumentation and General Methods

All primers used for DNA amplifications and DNA sequencing services were provided by Gene Technologies Lab (GTL) at Texas A&M University. Protein

concentrations were analyzed via Bradford method (Standard: Bovine serum albumin with linear range of 0.5 mg/mL to 5 mg/mL). Primers, plasmids and strains used in this study are listed in Table 6. The map of the plasmid constructs is presented in Appendix Figure 9.

**Table 6** Primers, plasmids and strains used in the AziH1, AziH2 and AziH3 studies.

| **Primer/ plasmid/ strain** | **Description** | **Source** |
|---|---|---|
| **Primers** | | |
| *aziH1_ EcoR*I_F | CCGAATTCAAGCCGATGATCCTGTTCTC | This study |
| *aziH1_ Hind*III_R | CAAGCTTGAAGTACCCCTCACGCTTGC | This study |
| *aziH2_ EcoR*I_F | GGCGAATTCATGAGTGGATCCACCGGACGGTGG | This study |
| *aziH2_ Hind*III_R | CAAGCTTGCCGGTGACGGCCGCGCC | This study |
| *aziH3_EcoR*I_F | GGGAATTCATGATCGGGCCTGAATCATGTG | This study |
| *aziH3_Hind*III_R | GGAAGCTTTGCCACGAACCGCTTCCG | This study |
| **Plasmids** | | |
| pGEM-T easy | Sub-cloning vector, *E. coli* | Promega |
| pET-24b | T7 expression vector, C-terminal $His_6$-Tag, Kanamycin resistance | Novagen |
| pET24b-*aziH1* | *aziH1* gene (813 bp) was inserted at *EcoR*I and *Hind*III sites | This study |
| pET21a-*aziH2* | *aziH2* gene (1308 bp) was inserted at *EcoR*I and *Hind*III sites | This study |
| pET24b-*aziH3* | *aziH3* gene (558 bp) was inserted at *EcoR*I and *Hind*III sites | This study |
| **Strains** | | |
| *E. coli* DH10B | Cloning host | Invitrogen |
| *E. coli* BL21(DE3) | Protein expression host | Invitrogen |

**Cloning, Protein Overexpression, and Purification of AziH1, AziH2 and AziH3**

*aziH1*, *aziH2*, and *aziH3* were individually cloned in vector pET-24b. The construct was transformed in BL21(DE3) *E. coli* strain for protein overexpression. A 5 mL overnight culture in LB media containing 50 µg/mL kanamycin was added to 1L media and grown till an $OD_{600}$ of 0.8. The culture was induced with 1 mM IPTG and incubated at 16 °C for 22-24 hours prior to harvest. The cells were centrifuged at 6,000×g for 20 min, washed twice with cold 50 mM phosphate buffer (300 mM NaCl and 10% glycerol at pH 7) and re-suspended in the same buffer containing 1 mM dithiothreitol (DTT) and 1 mM phenyl methylsulfunyl fluoride (PMSF). The cell pellets were sonicated on ice water bath using Branson Sonifier 450 (Branson Ultrasonics) fitted with a micro tip, output setting 6, duty cycle 50%, for 8 cycles for 30 sec each and centrifuged for 1 h at 12,000×g.

The soluble protein was purified by Nickel affinity chromatography, His Trap ™ FF 5 ml column (GE Healthcare Life Sciences), according to the instructions provided by the supplier. The purified fractions were desalted and concentrated using Amicon® 10K Ultra centrifugal filter (EMD Millipore).

# CHAPTER V

## CONCLUSION

Advancement in bioinformatics and high-throughput compound screening accelerated the process of identifying new and valuable natural compounds. The studies on newly isolated natural products' biosynthesis also reveal interesting chemical pathways and novel reactions. Since drug design predominately relies on structural modification and optimization of existing compounds, refine understanding of the structural origins of various classes of natural products and their related biosynthesis will undoubtedly improve natural product-based drug development in the future.

Azinomycin B, a secondary metabolite isolated from *Streptomyces sahachiroi*, exhibits excellent antitumor activity and mode of action through its rare and complex structural makeup. The compound's aziridine and epoxide moieties are responsible for its promising bioactivity via dsDNA interstrand crosslinks in selected tumor types. Understanding the biosynthetic process of these unique structural aspects of azinomycin B offers important insights towards its *in vivo* activities as well as target specificity. Therefore, we aim to characterize the important biosynthetic pathways of azinomycin B at the mechanistic level. Although it is extremely challenging to completely map out azinomycin B's biosynthetic routes experimentally, the use of bioinformatics had helped us narrow down the putative components required in each step of the biosynthesis.

AziW catches our attention when the *in vitro* and *in vivo* studies of AziC2 were inconclusive and suggested a possible existence of a partner protein. Through a series of

*in vitro* isotope-feeding experiments, AziW was proven to play a role in the assembly of azinomycin B's azabicycle moiety during the natural product's biosynthesis. The next step in this project includes the use of mass spectrometry to corroborate our experimental observation and strengthen our hypothesis.

Our research interest in the azabicycle moiety includes the genes downstream of *aziC2*. This particular biosynthetic route contains many unknown steps such as the aziridine ring closure that we believe are chemically novel. In order to fully characterize the downstream biosynthetic reactions, we have to investigate the pathway sequentially. Since we have successfully proved the function of AziC3 (N-acetylglutamate kinase) and AziC4 (N-acetyl-γ-glutamyl-phosphate reductase), which frequently work together to convert the γ-carboxylic acid group of N-acetylglutamate to an aldehyde, we expect to find a downstream N-acetyl-dihydroxyketone to complete the biosynthesis of the azabicycle. Essentially, the complete characterization of the azabicycle biosynthesis can broaden the understanding of azinomyicin B's mode of action.

## REFERENCES


1. Newman, D. J. and Cragg, G. M. Natural products as sources of new drugs over the 30 years from 1981 to 2010. *J. Nat. Prod.* **75**, 311-335 (2012).
2. Newman, D. J. Natural products as leads to potential drugs: An old process or the new hope for drug discovery? *J. Med. Chem.* **51**, 2589-2599 (2008).
3. da Rocha, A. B., Lopes, R. M., and Schwartsmann, G. Natural products in anticancer therapy. *Current Opinion in Pharmacology* **1**, 364-369 (2001).
4. Wani, M. C., Taylor, H. L., Wall, M. E., Coggon, P. and McPhail, A.T. Plant antitumor agents. VI. Isolation and structure of taxol, a novel antileukemic and antitumor agent from Taxus brevifolia. *J. Am. Chem. Soc.* **93**, 2325-2327 (1971).
5. Fuchs, D. A. and Johnson, R. K. Cytologic evidence that taxol, an antineoplastic agent from Taxus brevifolia, acts as a mitotic spindle poison. *Cancer Treat. Rep.* **62**, 1219-1222 (1978).
6. Sehgal, S. N., Baker, H. and Vezina, C. Rapamycin (AY-22, 989), a new antifungal antibiotic II. Fermentation, isolation and characterization. *The Journal of Antibiotics* **XXVIII No. 10**, 727-732 (1975).
7. Gao, X., Xie, X., Pashkov, I., Sawaya, M. R., Laidman, J., Zhang, W., Cacho, R., Yeates, T. O. and Tang, Y. Directed evolution and structural characterization of a simvastatin synthase. *Chemistry & Biology* **16**, 1064-1074 (2009).

8. Schwartsmann, G., da Rocha, A. B., Berlinck, R. GS. And Jimeno, J. Marine organisms as a source of new anticancer agents. *Lancet Oncol.* **2**, 221-225 (2001).
9. Hata, T., Koga, F., Sano, Y., Kanamori, K., Matsumae, A. *et al.* Carzinophilin, a new tumor inhibitory substance produced by *Streptomyces*, I. *J. Antibiot. Ser. A* **7**, 107-112 (1954).
10. Ishii, T., Sato, Y., Hatori, T., Fukui, T., Kubouchi, K., Noguchi, T., Sukigara, K., and Takeischi, T. (1956). The clinical and histological studies on the cases treated by carzinophilin. Gan 47, 360-363.
11. Onda, M., Konda, Y. and Noguchi, A. Revised structure for the naphthalenecarboxylic acid from carzinophilin. *J. Antibiot.* **XXII**, 1, 42-44 (1969).
12. Tanaka, M., Kishi, T., and Maruta, Y. Carzinophilin, Part I. The structure of methanolysis product. *J. Antibiot*. **13**, 361-364 (1959).
13. Tanaka, M., Kishi, T., and Maruta, Y. Carzinophilin, Part II. The structure of methanolysis product. *J. Antibiot.* **13**, 177-181 (1960).
14. Onda, M., Konda, Y., Omura, S. and Hata, T. Structure of carzinophilin II. A new amino acid and its derivative from carzinophilin. *Chem. Pharm. Bull.* **19**, 10, 2013-2019 (1971).
15. Lown, J. W. and Hanstock, C. C. Structure and function of the antitumor antibiotic carzinophilin A: The first natural intercalative bisalkylator. *J. Am. Chem. Soc.* **104**, 3213-3214 (1982).

16. Onda, M., Konda, Y., Hatano, A., Hata, T. and Omura, S. Structure of carzinophilin. IV. Structure elucidation by nuclear magnetic resonance spectroscopy. *Chem. Pharm. Bull.* **32**, 8, 2995-3002 (1984).
17. Nagaoka, K., Mastumoto, M., Ono, J., Yokoi, K., Ishizeki, S. and Nakashima, T. J. Carzinophilin is identical with azinomycin B which was isolated from cultures of *Streptomyces* griseofuscus. *J. Antibiot.* **39**, 1527 (1986).
18. Zhou, Z., Gu, J., Du, Y., Li, Y. and Wang, Y. The –omics era- toward a systems-level understanding of *Streptomyces*. *Current genomics* **12**, 404-416 (2011).
19. Chater, K. F. *Streptomyces* inside-out: a new perspective on the bacteria that provide us with antibiotics. *Phil. Trans. R. Soc. B* **361**, 761-768 (2006).
20. Foster, J. W. and Katz, E. Control of actinomycin D biosynthesis in *Streptomyces parvullus*: regulation of tryptophan oxygenase activity. *J. Bacteriol.* **148**, 2, 670-677 (1981).
21. Kino, T., Hatanaka, H., Hashimoto, M., Nishiyama, M., Goto, T., Okuhara, M., Kohsaka, M., Aoki, H. and Imanaka, H. FK-506, a novel immunosuppressant isolated from a *Streptomyces*. I. Fermentation, isolation, and physico-chemical and biological characteristics. *J. Antibiot.* **XL**, 9, 1249-1255 (1987).
22. Donadio, S., Sosio, M. and Lancini, G. Impact of the first Streptomyces genome sequence on the discovery and production of bioactive substances. *Appl Microbiol Biotechnol* **60**, 377-380 (2002).
23. Omura, S., Ikeda, H., Ishikawa, J., Hanamoto, A., Takahashi, C., Shinose, M., Takahashi, Y., Horikawa, H., Nakazawa, H., Osonoe, T., Kikuchi, H. Shibai, T.,

Sakaki, Y. and Hattori, M. Genome sequence of an industrial microorganism Streptomyces avermitilis: Deducing the ability of producing secondary metabolites. *PNAS* **98**, 21, 12215-12220 (2001).

24. Lawson, D. M. and Stevenson, C. E. M. Structural and functional dissection of aminocoumarin antibiotic biosynthesis: a review. *J. Struct. Funct. Genomics* **13**, 125-133 (2012).
25. Yokoi, K., Nagaoka, K., Nakashima, T. Azinomycins A and B, new antitumor antibiotics. II. Chemical structures. *Chem. Pharm. Bull.* **34**, 4554-4561 (1986).
26. Nagaoka, K., Matsumoto, M., Oono, J., Yokoi, K., Ishizeki, S., Nakashima, T. Azinomycins A and B, new antitumor antibiotics. I. Producing organism, fermentation, isolation, and characterization. *J. Antibiot. (Tokyo)* **39**, 11, 1527-1532 (1986).
27. Ishizeki, S., Ohtsuka, M., Kazuhiko, I., Kukita, K.-I., Nagaoka, K., Nakashima, T. Azinomycins A and B, new antitumor antibiotics. III. Antitumor activity. *J. Antibiot. (Tokyo)* **40**, 1, 60-65 (1987).
28. Shimada, N., Uekusa, M., Tosiro, D., Ishu, Y., Iizuka, T., Sato, Y., Hatori, T., Fulio, T., Sudo, M. Clinical studies of carzinophilin, an antitumor substance. *J. Antibiot. (Tokyo)* **8**, 67-76 (1955).
29. Lown, J. W., Majumdar, K. C. Studies related to antitumor antibiotics. Part IX. Reactions of carzinophillin with DNA assayed by ethidium fluorescence. *Can. J. Biochem.* **55**, 630-635 (1977).

30. Fujiwara, T., Saito, I., Sugiyama, H. Highly efficient DNA interstrand crosslinking induced by an antitumor antibiotic, Carzinophilin. *Tetrahedron Lett.* **40**, 2, 315-318 (1999).

31. Armstrong, R. W., Salvati, M. E., Nguyen, M. Novel interstrand cross-links induced by the antitumor antibiotic carzinophilin/azinomycin B. *J. Am.Chem. Soc.* **114**, 8, 3144-3145 (1992).

32. Zhao, Q., He, Q., Ding, W., Tang, M., Kang, Q., Yu, Y., Deng, W., Zhang, Q., Fang, J., Tang, G., Liu, W. Characterization of the azinomycin B biosynthetic gene cluster revealing a different iterative type I polyketide synthase for naphthoate biosynthesis. *Chemistry & Biology* **15**, 693-705 (2008).

33. Corre C. and Lowden P.A. The first biosynthetic studies of the azinomycins: acetate incorporation into azinomycin B. *Chem. Commun.* **8**, 990-991 (2004).

34. Corre C., Landreau C. A., Shipman M. and Lowden P. A. Biosynthetic studies on the azinomycins: the pathway to the naphthoate fragment. *Chem. Commun.* **22**, 2600-2601 (2004).

35. Sharma V., Kelly G. T., Foulke-Abel J. and Watanabe C. M. Aminoacetone as the penultimate precursor to the antitumor agent azinomycin A. *Org. Lett.* **17**, 4006-4009 (2009).

36. Sharma V., Kelly G. T. and Watanabe C. M. Exploration of the molecular origin of the azinomycin epoxide: timing of the biosynthesis revealed. *Org. Lett.* **21**, 4815-4818 (2008).

37. Ding W., Deng W., Tang M., Zhang Q., Tang G., Bi Y. and Liu W. Biosynthesis of 3-methoxy-5-methyl naphthoic acid and its incorporation into the antitumor antibiotic azinomycin B. *Mol. Biosyst.* **6**, 1071-1081 (2010).

38. Foulke-Abel J., Kelly G. T., Zhang H. and Watanabe C. M. Characterization of AziR, a resistance protein of the DNA cross-linking agent azinomycin B. *Mol. Biosyst.* **9**, 2563-2570 (2011).

39. Wang S., Zhao R., Liu K., Zhu M., Li A. and He J. Essential role of an unknown gene aziU3 in the production of antitumor antibiotic azinomycin B verified by utilizing optimized genetic manipulation systems for Streptomyces sahachiroi. *Microbiol. Lett.* **2**, 147-154 (2012).

40. Takahashi I., Takahashi K., Ichimura M., Morimoto M., Asano K., Kawamoto I., Tomita F. and Nakano H. Duocarmycin A, a new antitumor antibiotic from Streptomyces. *J. Antibiot.* (Tokyo) **41**, 12, 1915-1917 (1988).

41. Tomasz M., Chawla A.K. and Lipman R. Mechanism of monofunctional and bifunctional alkylation of DNA by mitomycin C. *Biochemistry* **27**, 9, 3182-3187 (1988).

42. Seto H. and Yonehara H. Studies on the biosynthesis of pentalenolactone. III. Isolation of a biosynthetic intermediate hydrocarbon, pentalenene. *J. Antibiot.* (Tokyo) **33**, 1, 92-93 (1980).

43. Argoudelis A. D., Reusser F., Whaley H. A., Baczynskyj L., Mizsak S. A. and Wnuk R. J. Antibiotics produced by Streptomyces ficellus. I. Ficellomycin. *J. Antibiot.* (Tokyo) **29**, 10, 1001-1006 (1976).

44. Kellogg B. A. and Poulter C. D. Chain elongation in the isoprenoid biosynthetic pathway. *Curr. Opin. Chem. Biol.* **1**, 4, 570-578 (1997).

45. Blagg B. S., Jarstfer M. B., Rogers D. H. and Poulter C. D. Recombinant squalene synthase. A mechanism for the rearrangement of presqualene diphosphate to squalene. *J. Am. Chem. Soc.* **124**, 30, 8846-8853 (2002).

46. Thibodeaux C. J., Chang W.C. and Liu H. W. Enzymatic chemistry of cyclopropane, epoxide, and aziridine biosynthesis. *Chem. Rev.* **112**, 3, 1681-1709 (2012).

47. Sono M., Roach M. P., Coulter E. D. and Dawson J. H. Heme-Containing Oxygenases. *Chem. Rev.* **96**, 7, 2841-2888 (1996).

48. Shaik S., Hirao H. and Kumar D. Reactivity patterns of cytochrome P450 enzymes: multifunctionality of the active species, and the two states-two oxidants conundrum. *Nat. Prod. Rep.* **24**, 3, 533-553 (2007).

49. Zhu Y. and Silverman R. B. Revisiting heme mechanisms. A perspective on the mechanisms of nitric oxide synthase (NOS), Heme oxygenase (HO), and cytochrome P450s (CYP450s). *Biochemistry* **47**, 8, 2231-2243 (2008).

50. Bicker U. and Fischer W. Enzymatic aziridine synthesis from beta amino-alcohols--a new example of endogenous carcinogen formation. *Nature* **249**, 455, 344-345 (1974).

51. Foulke-Abel J., Agbo H., Zhang H., Mori S. and Watanabe C. M. Mode of action and biosynthesis of the azabicycle-containing natural products azinomycin and ficellomycin. *Nat. Prod. Rep.* **28**, 4, 693-704 (2011).

52. Kelly G. T., Sharma V. and Watanabe C. M. An improved method for culturing Streptomyces sahachiroi: biosynthetic origin of the enol fragment of azinomycin B. *Bioorg. Chem.* **36**, 1, 4-15 (2008).

53. Horie A., Tomita T., Saiki A., Kono H., Taka H., Mineki R., Fujimura T., Nishiyama C., Kuzuyama T. and Nishiyama M. Discovery of proteinaceous N-modification in lysine biosynthesis of Thermus thermophilus. *Nat. Chem. Biol.* **5**, 9, 673-679 (2009).

54. Haas D., Leisinger T. N-acetylglutamate 5-phosphotransferase of Pseudomonas aeruginosa. Purification and ligand-directed association-dissociation. *Eur. J. Biochem.* **52**, 2, 365-375 (1975).

55. Kittigowittana, K., Yang, C. T., Cheah, W. C., Chuang, K. H., Tuang, C, Y., Chang, Y. T., Golay, X. and Bates, R. W. Development of intravascular contrast agents for MRI using gadolinium chelates. *ChemMedChem* **6**, 781-787 (2011).

56. Chodounska, H. *et al. U.S. Patent PCT/CZ2010/000065* **134** (2010).

57. Takahara K., Akashi K. and Yokota A. Continuous spectrophotometric assays for three regulatory enzymes of the arginine biosynthetic pathway. *Anal. Biochem.* **368**, 2, 138-147 (2007).

58. Cummings J., Spanswick V. J. and Smyth J. F. Re-evaluation of the molecular pharmacology of mitomycin C. *Eur. J. Cancer* **31A**, 12, 1928-1933 (1995).

59. Sugiura Y., Shiraki T., Konishi M. and Oki T. DNA intercalation and cleavage of an antitumor antibiotic dynemicin that contains anthracycline and enediyne cores. *Proc. Natl. Acad. Sci. U S A.* **87**, 10, 3831-3835 (1990).

# APPENDIX

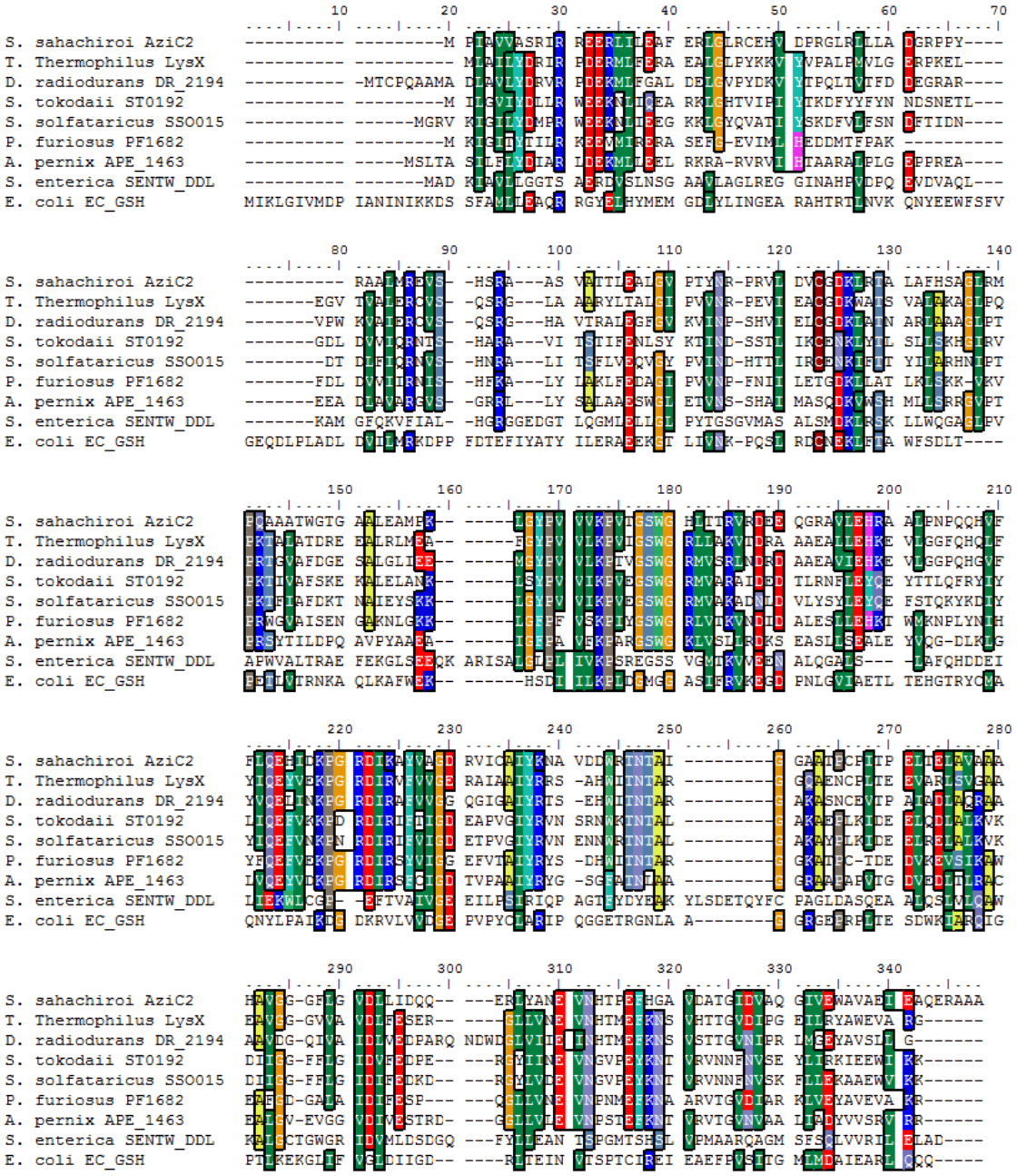


**Appendix Figure 1** Amino acid sequence alignment of AziC2 with LysX homologs.
Amino acid important for LysX and LysW interaction based on electrostatic surface mapping (red arrow).

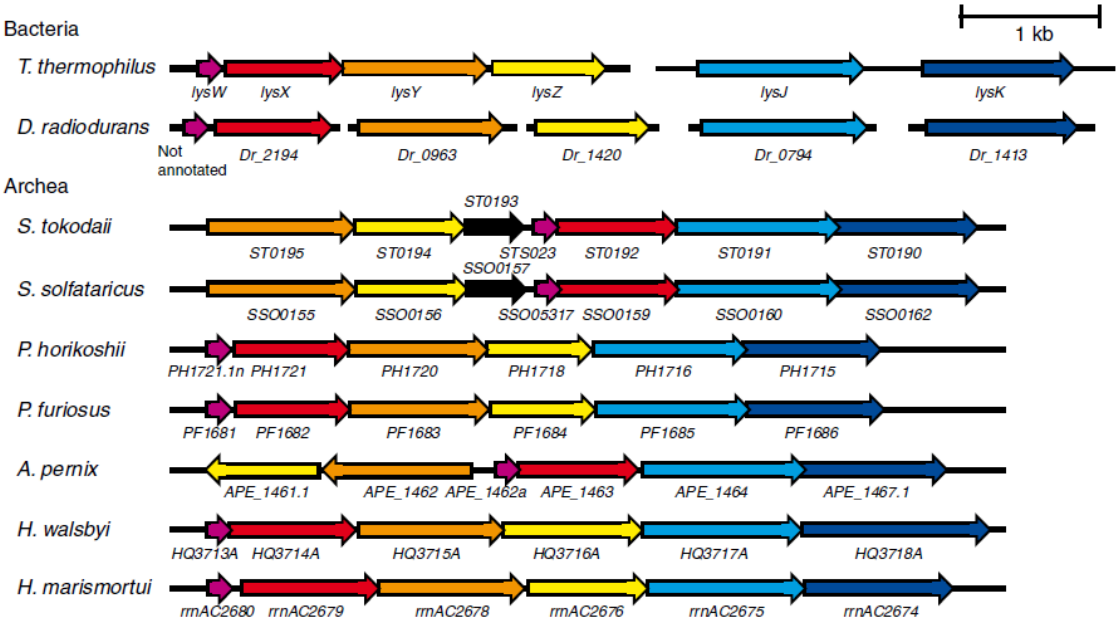


**Appendix Figure 2** Gene clusters of lysine biosynthetic enzymes from different species. Pink: LysW homologs; Red: LysX homologs; Orange: LysY homologs; Yellow: LysZ homologs; Blue: LysJ homologs; Navy: LysK homologs. **Adapted from** Horie *et al.* [53].

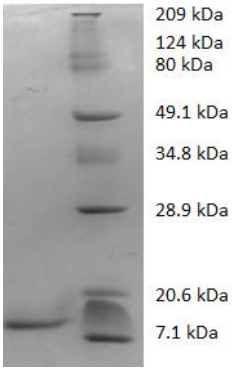


**Appendix Figure 3** SDS-PAGE of purified AziW.

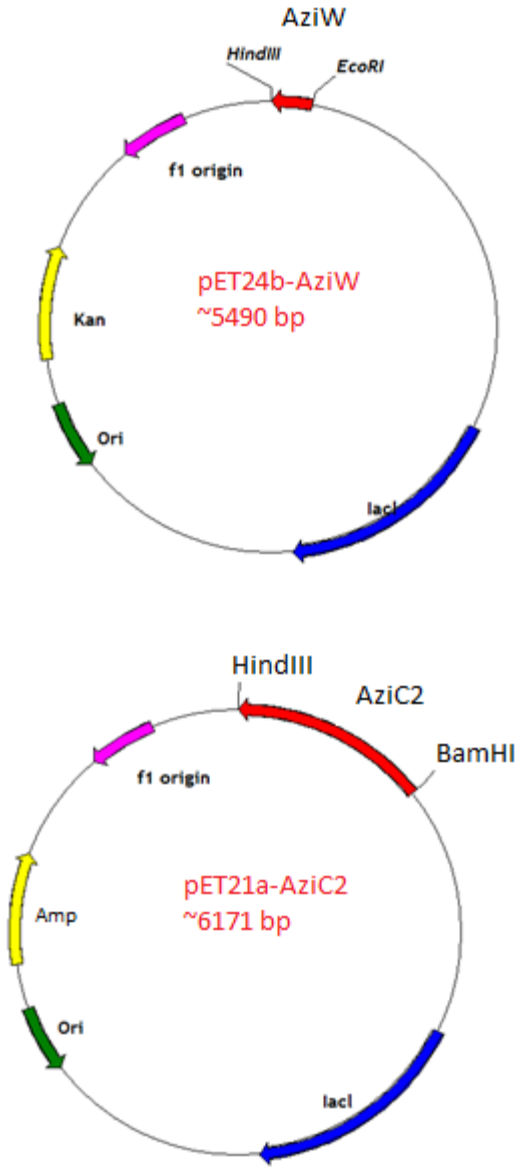


**Appendix Figure 4** *aziW*-pET24b and *aziC2*-pET24a constructs.

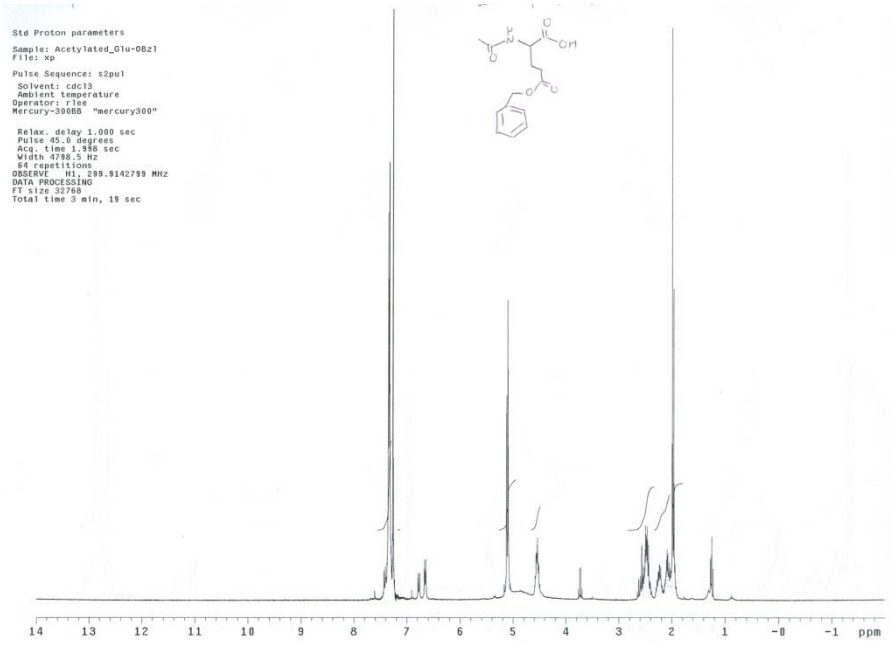


**Appendix Figure 5** $^{1}$H-NMR of acetylated glutamate-γ-benzyl ester.

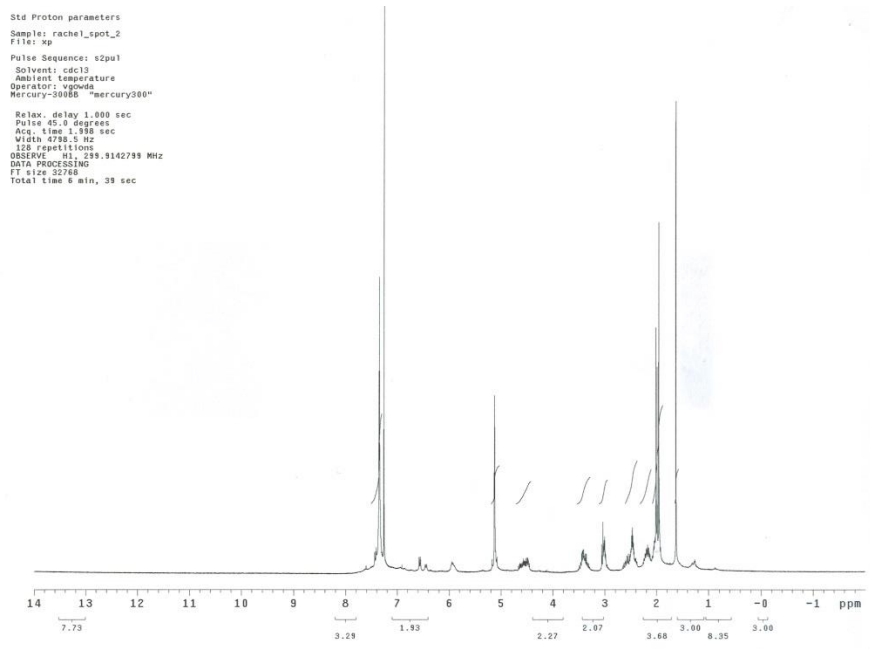


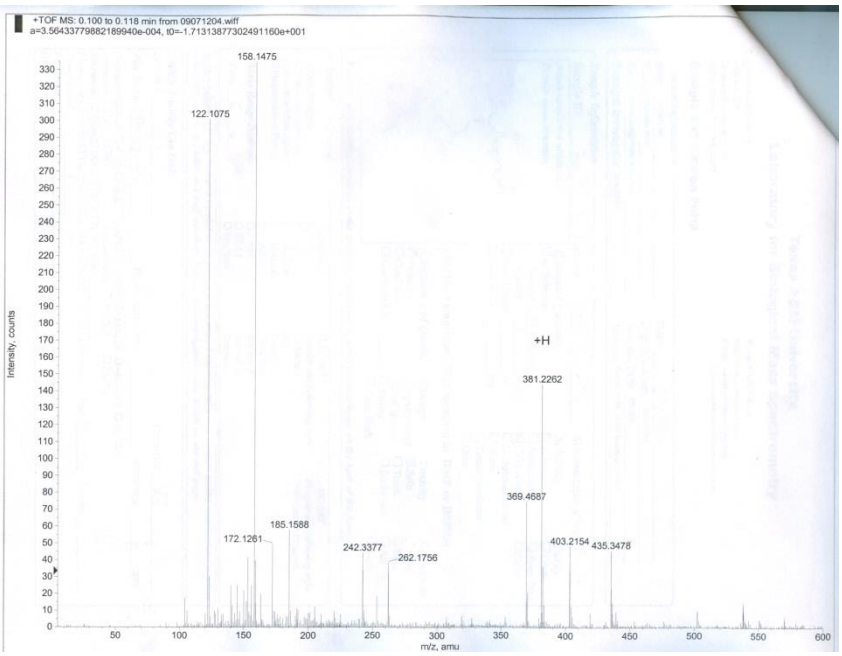


**Appendix Figure 6** $^{1}$H-NMR and mass spectrum of cysteamine-linked acetyl-glutamate-γ-benzyl ester.

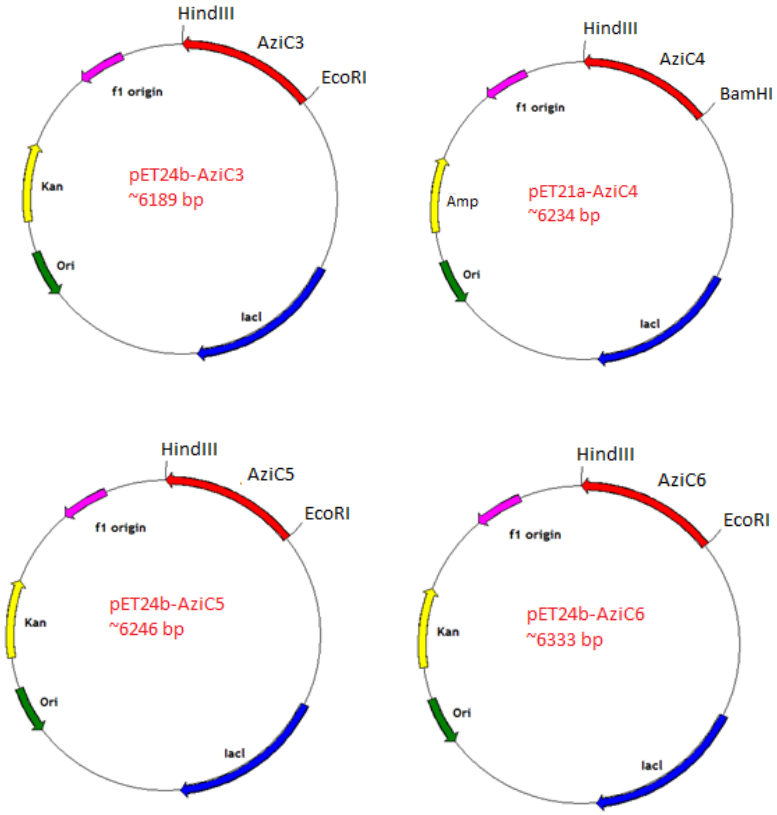


**Appendix Figure 7** *aziC3*-pET24b, *aziC4*-pET21a, *aziC5*-pET24b and *aziC6*-pET24b constructs.

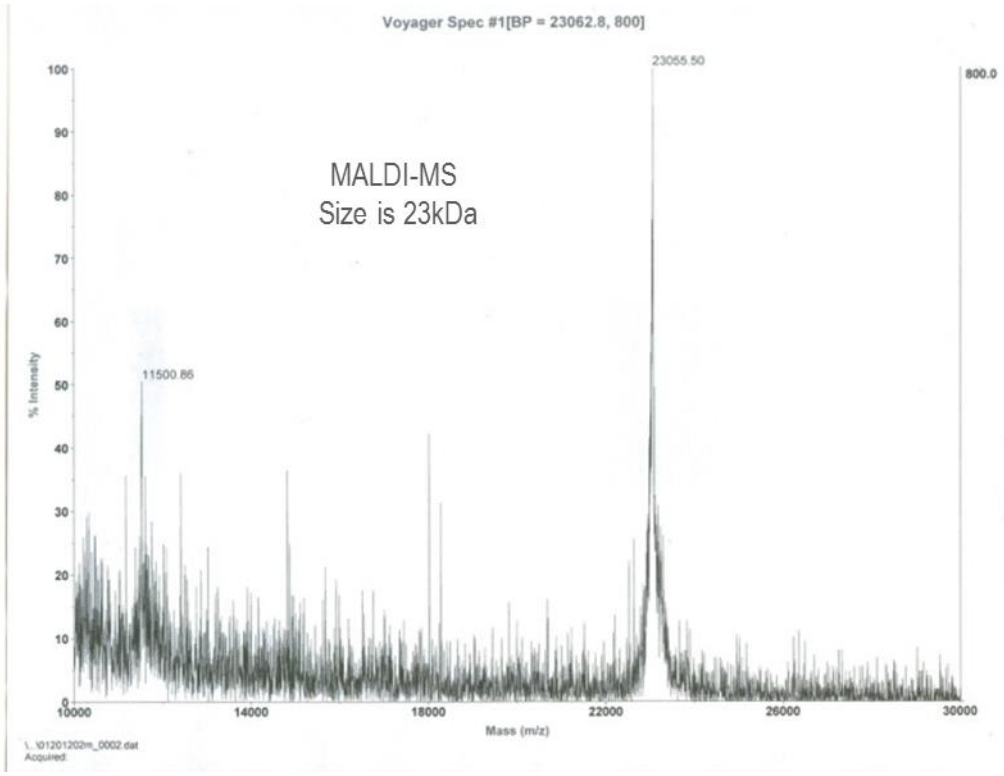


**Appendix Figure 8** MALDI-MS of AziH3.

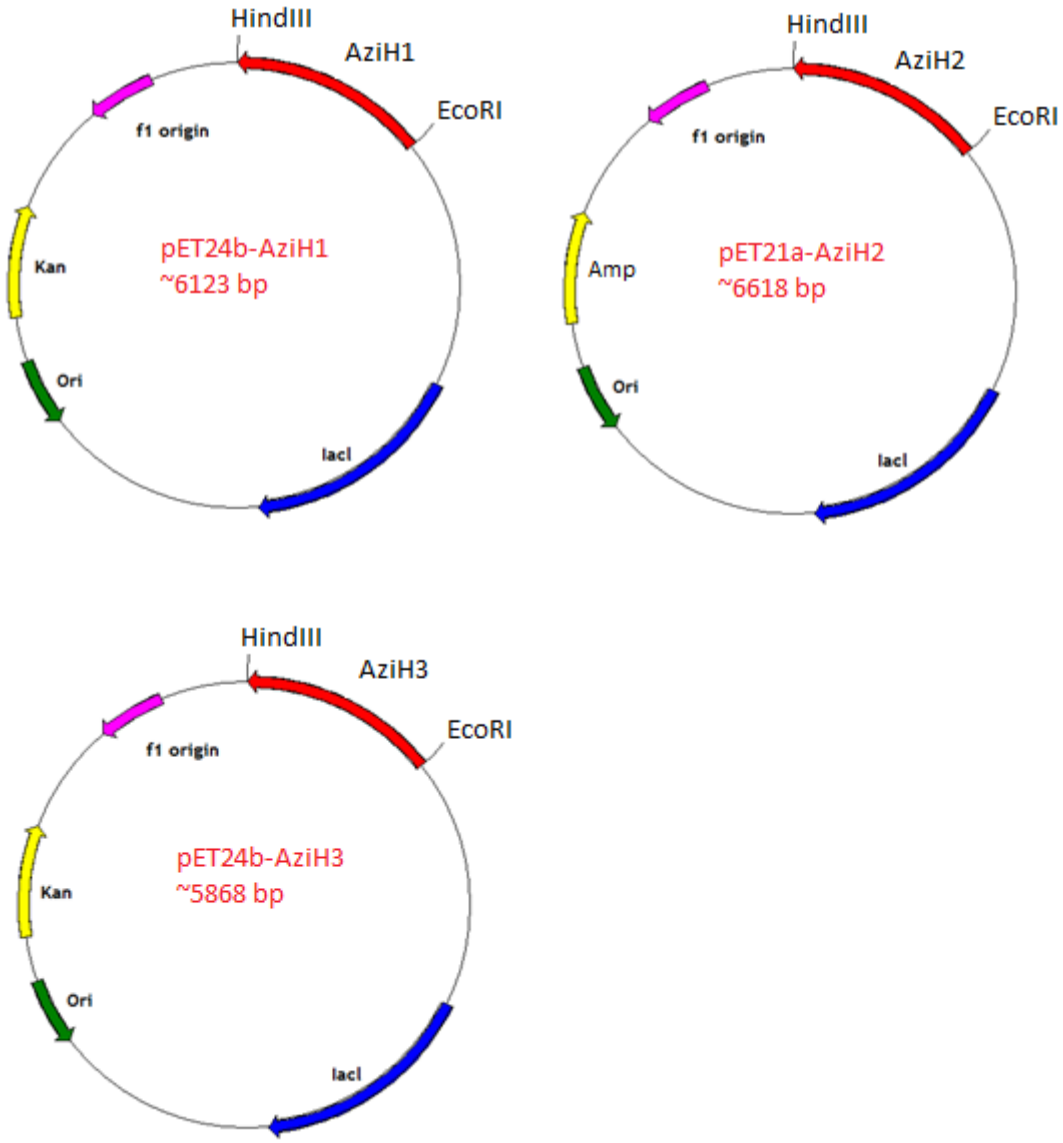


**Appendix Figure 9** *aziH1*-pET24b, *aziH2*-pET21a and *aziH3*-pET24b constructs.